People's Democratic Republic of Algeria
Ministry of Higher Education and Scientific Research
University M'Hamed BOUGARA – Boumerdes

Institute of Electrical and Electronic Engineering

Department of Electronics

Final Year Project Report Presented in Partial Fulfilment of
the Requirements for the Degree of

MASTER

In **Telecommunication**
Option: **Telecommunications**

Title:

Miniaturization of Ultra-Wide Band Bandpass Filter With Multiple Notches

Presented by:

- **MEDDAH Abderraouf**
- **MARICHE Abdelatif**

Supervisor:

Dr.F.MOUHOUCHE

Registration Number:...../2021

Abstract

As the ultra-wideband system (3.1GHz to 10.6GHz) is known to be easily interfered by narrow-band signals laying on the same frequency range, A compact ultra-wideband (UWB) band-pass filter (BPF) with multiple notches is presented in this work. The UWB -BP filter rejects two WLAN bands at 5.2GHz and 5.8GHz in addition to 7.2GHz for C band satellite signals when needed, due to the tuning ability property of the design. It consists of a modified dumbbell DGS unit with a feed line terminated by two H shapes to achieve the UWB band-pass characteristics. Next, two pairs of split ring resonators and a rectangular loop are added to create the WLAN and C band rejection respectively at a level higher than -17dB.

The proposed filter occupies an area of $30\times 15mm^2$. To confirm the theory a prototype is fabricated and its measured response is found to be in close agreement with the simulated response.

Keywords: Ultra Wide Band (UWB), Band-pass Filter (BPF), Defected Ground Structure (DGS), Split Ring Resonators (SRR);

Acknowledgment

☺ First and foremost, we thank Allah, the most gracious, the most merciful for his help to finish this modest work.

☺ We place on record our sincere thanks and appreciation to our supervisor Dr.F.MOUHOUCHE for sharing expertise and valuable guidelines which were of an extreme help to us.

☺ We acknowledge, with gratitude and appreciation, to all members of the Department of telecommunications specifically and electronics in general, for their encouragement and support.

☺ We wish to express our thanks and gratitude to our parents, the ones who can never ever be thanked enough, for the overwhelming love and care they bestow upon us, we would say that after Allah, without you, it was never possible to finish our study careers.

☺ Finally, thanks to everyone who helped even with a prayer to make this work successful

dedication

First and foremost

All praise is to « Allah » the Almighty for his assistance in finishing this graduation project.

I'd like to dedicate this dissertation

To my beloved parents who were always there for me.

To my brothers and sister for their support.

To my family, friends and all people in my life.

Abderraouf MEDDAH

dedication

I'd like to dedicate my work

To my family, especially to my lovely parents for supporting and encouraging me during all my study career.

To my sister “Sarah” and brother “Yasser”.

To all my family and friends whom I spent nice moments especially my best friends M.Abdeldjalil, S.Abdeldjalil, Nadjib, Hamza and Abdelali.

Abdelatif MARICHE

Table of content

CHAPTER I: MICROWAVE FILTERS AND DGS TECHNIQUE

Table of content

CHAPTER II: UWB TECHNOLOGY AND FILTERS

Table of content

CHAPTER III: DESIGN OF UWB BAND PASS FILTER WITH MULTIPLE NOTCHES

List of figures

List of figures

List of tables

List of abbreviations

BPF	**Bandpass Filter**
BSF	**Band Stop Filter**
BW	**Bandwidth**
CPW	**Coplanar waveguide**
CST	**Computer Simulation Technology**
DGS	**Defected Ground Structure**
FBW	**Fractional bandwidth**
FCC	**Federal Communications Commission**
GPS	**Global Positioning**
HPF	**High Pass Filter**
IEEE	**Institute of Electrical and Electronics Engineering**
IL	**Insertion Loss**
ISM	**Industrial, scientific and medical**
ITT	**International Telephone and Telegraph**
LOS	**Line-of-sight**
LPF	**Low Pass Filter**
LTC	**Low Temperature Co-fired Ceramic**
LTI	**Linear Time-invariant**
MMR	**Multi-mode resonator**
NLOS	**Non-line-of-sight**
PBG	**Photonic Band Gap**
RF	**Radio Frequency**
RL	**Return Loss**
SIW	**Substrate Integrated Waveguide**
TEM	**Transverse Electromagnetic**
TF	**Transfer Function**
UWB	**Ultra wide band**

List of abbreviations

VNA	**Vector Network Analyzer**
WLAN	**Wireless Local Area Network**

List of symbols

F_c	Center frequency
F_L	Low frequency
F_H	High frequency
dB	Decibels
F_{cutoff}	Cutoff frequency
Q	Quality factor
Hz	Hertz
m	meters
mm	millimeters
L	Inductance
C	Capacitance
R	Resistance
π	Pi number
$Z0$	Characteristic impedace
λg	Guided wavelength
$\lambda 0$	Free space wavelength
c	Light speed
V_p	Phase velocity
P_{ref}	Reflected power
P_{in}	Input power
t	Thickness
W	Width
mW	milliwatt

List of symbols

$f_n(w)$	Characteristic function
εeff	Effective dielectric constant
εr	Relative dielectric

General Introduction

RF Filters are key components in telecommunication since the early stages, and have evolved significantly with the growth of communication technologies. The introduction of carrier telephony, which required a new technology capable of extracting and detecting signals confined within a certain band, expedited the development of filter technology.

The rapid growth of communication system raises the demand for filters with specified characteristics, such as good spurious free response, narrow/wide bandwidth, and good in band performance at a low cost and small size. There are various types of filters, one of which is the band pass filter (BPF). A BPF chooses a specific band of frequencies termed its pass-band and rejects all other frequencies.

The aim of this project is to design a microstrip BPF for UWB, then feed it with multiple notches in order to avoid interferences caused by other applications occupying the same frequency range. The used substrate material has a relative dielectric constant of 3.38, a thickness of 0.813 mm, copper thickness of 0.035 mm and a loss tangent of 0.0027. The design and simulation are carried using CST software, while the realization and measurements are done with the help of MITS Electronics PCB prototyping machine and Rohde& Schwarz VNA respectively.

The outlines of the report are organized as follows:

A literature review about filters and DGS technique are presented in Chapter 1. Chapter 2 introduces UWB technology. In addition to the development of UWB band pass Filters.

Chapter 3 investigates the simulation and design steps of the proposed UWB BPF filter before and after the addition of multiple notches and ends up with the fabrication, measurements and comparison to similar works

Finally, a conclusion and some suggestions for future scope are presented.

CHAPTER I

MICROWAVE FILTERS AND DGS TECHNIQUE

I.1 Introduction

The demand for RF and microwave filters has increased as the scope of current wireless communication applications and radar systems has grown in today's technology, as they play an essential role in transmit-receive systems. Radio and television broadcasting, mobile and satellite communications, traffic radar, air traffic radar are just a few examples.

The microwave and RF filters are frequency selective networks with two ports. The filter's primary function is to reject undesired signal frequencies while allowing good transmission of needed frequencies. The fundamental theory of microwave filters is well defined to describe how to construct actual microwave filters and examine how to implement high-performance filters for modern communication systems.

I.2 RF/Microwave filter types

I.2.1 Low pass filter (LPF)

A low pass filter (LPF) is a filter that selects low frequencies up to the cut-off frequency f_c and attenuates other frequencies which are higher than f_c. The LPFs are used whenever high frequencies be removed from a signal and they are employed in applications requiring the rejection of high frequency signals such as in modern microwave communication systems, radar and satellite communication system. Figure I.1 Shows the response of an LPF with its cut-off frequency

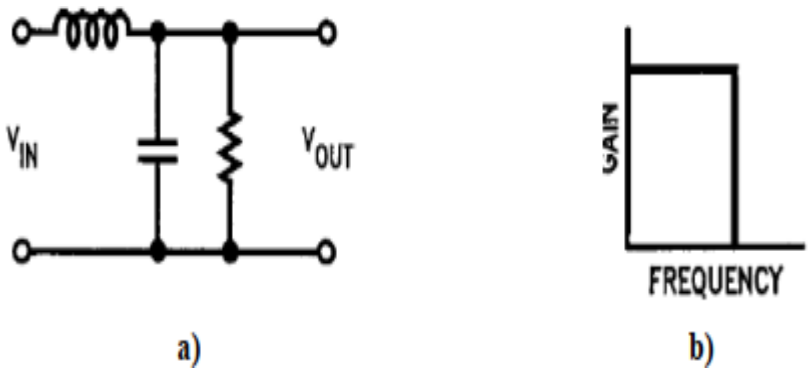

Figure I.1 An ideal LPF: a) Equivalent Circuit and b) Frequency Response [1]

I.2.2 High pass filter (HPF)

The high-pass filter is quite the inverse of the low pass filter. It attenuates signals having lower frequencies than the cut-off frequency and passes the signals with higher frequencies. HPF can be used in loud speakers to reduce the low level noise. It can also be used to eliminate rumble distortion in audio application. Figure I.2 shows the response of an HPF.

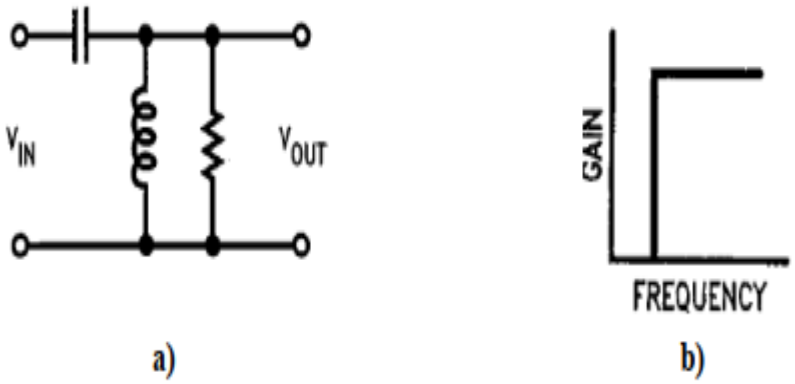

Figure I.2 An ideal HPF: a) Equivalent Circuit and b) Frequency Response [1]

I.2.3 Band pass filter (BPF)

A band-pass filter has a pass band between two cut-off frequencies f_H and f_L any input frequency outside this pass band is attenuated. There are two types of BPFs, wideband filters which are characterized by a low Q-factor (Q<10), and narrowband filters which have a high Q-factor (Q>10).Figure I.3 below shows both wideband and narrowband responses.

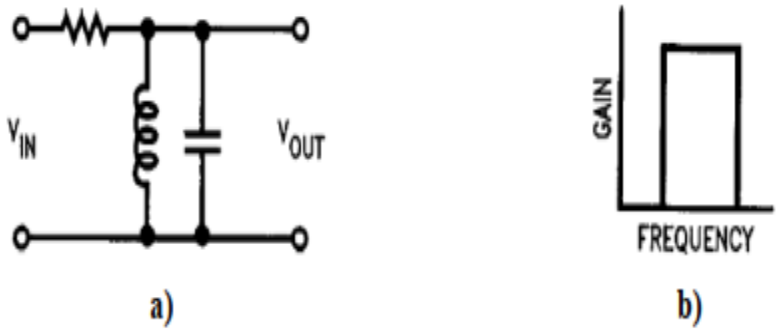

Figure I.3 An ideal BPF: a) Equivalent Circuit and b) Frequency Response [2]

I.2.4 Band stop filter (BSF)

The band-stop filter also called a band reject filter. In this filter frequencies are attenuated in the stop band while they are passed outside this band. The response of BSF is shown in the following Figure I.4.

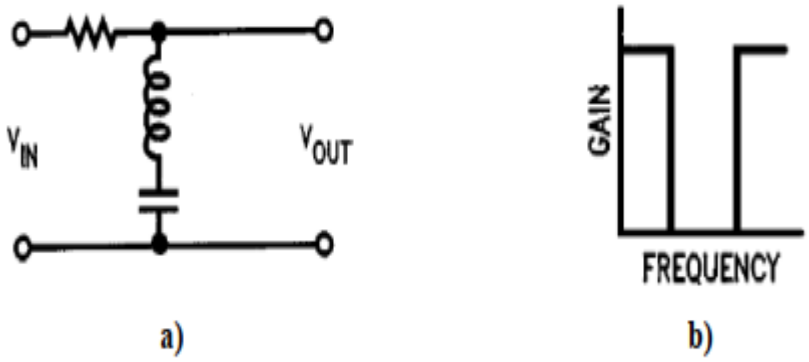

Figure I.4 An ideal BSF: a) Equivalent Circuit and b) Frequency Response [2]

I.3 Scattering parameters

S-parameters have earned a prominent position in RF circuit design, analysis and measurement. Scattering parameters (S-parameters) are defined and measured with ports terminated in a reference impedance. Modern network analyzers are well suited for accurate measurement of S-parameters. S-parameters have the additional advantage that they relate directly to important system specifications such as gain and return loss.

Two-port S-parameters are defined by considering a set of voltage waves. When a voltage wave from a source is incident on a network, a portion of the voltage wave is transmitted through the network, and a portion is reflected back toward the source. Incident and reflected voltage waves may also be present at the output of the network. New variables are defined by dividing the voltage waves by the square root of the reference impedance. The square of the magnitude of these new variables may be viewed as traveling power waves.

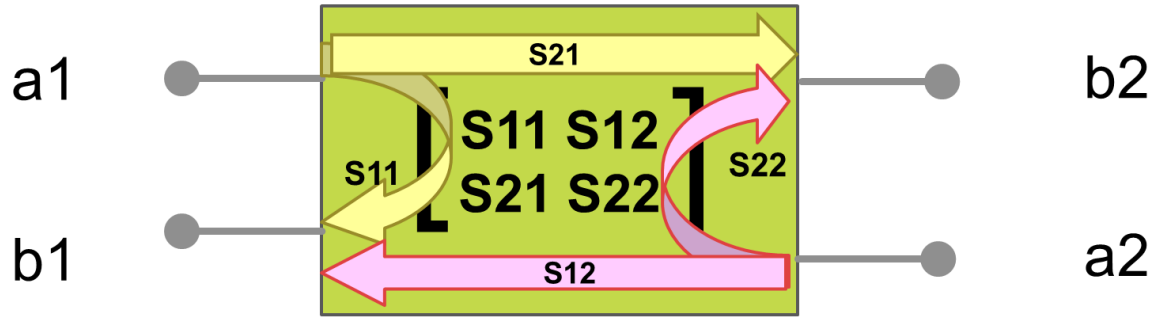

Figure I.5 Representation of two-port S-parameter reflection and transmission

- $|a_1|^2$=incident power wave at the network input
- $|b_1|^2$=reflected power wave at the network input
- $|a_2|^2$=incident power wave at the network output
- $|b_2|^2$=reflected power wave at the network output

These new variables and the network S parameters are related by the expressions

$$b_1=a_1S_{11}+a_2S_{12} \quad \text{(I.1)}$$

Which yields to:

$$S_{11} = b_1/a_1 \quad \text{When: } a_2=0 \quad \text{(I.2)}$$

$$S_{12} = b_1/a_2 \quad \text{When: } a_1=0 \quad \text{(I.3)}$$

$$S_{21} = b_2/a_1 \quad \text{When: } a_2=0 \quad \text{(I.4)}$$

$$S_{22} = b_2/a_2 \quad \text{When: } a_1=0 \quad \text{(I.5)}$$

Where:

- **S_{11}** is the reflection coefficient.
- **S_{12}** is the reverse transmission gain.
- **S_{21}** describes the forward transmission coefficient (insertion) gain.
- **S_{22}** is the output reflection coefficient of the device.

For some components and circuits, the scattering parameters can be calculated using network analysis techniques. Otherwise, the scattering parameters can be measured directly with a vector network analyzer (VNA) for one or two-port microwave network.

I.4 Basic concepts of filters

I.4.1 Transfer function

Transfer function is an essential feature used in analyzing electronic systems, such as signal processing, communication systems. In a two-port filter network, the network response characteristics are described by the transfer function different mathematical laws called

filtering function, where the most used ones are: Butterworth and Chebyshev laws [3]. In RF/microwave systems, the transfer function is defined by using scattering parameter S21, but in general, the square of S21 magnitude is used instead of its magnitude only, so for a lossless passive filter network the TF is defined as [4]:

$$|S_{21}(J\omega)|^2 = \frac{1}{1+\varepsilon^2 F_n^2(\omega)} \quad \text{(I.6)}$$

Where **ω** represents a frequency variable, **ε** is the ripple constant and $\mathbf{F_n(\omega)}$ is the characteristic function.

I.4.2 Insertion loss

The insertion loss of a filter is the additional loss between the source and the load caused by the insertion of the filter compared to its absence. Insertion loss is equal to the sum of dielectric losses, copper losses and reflected losses which are caused by the power dissipated in dielectric materials, the power dissipated by the conductor and by the voltage standing wave ratios (VSWR). It is usually expressed in decibel (dB).

$$IL(dB) = -20\log_{10}|S_{21}| \quad \text{(I.7)}$$

I.4.3 Return loss

Return loss (RL) is the loss rate of the power reflected back from the load to the power transmitted into the line, in other words, it is the measure of the effectiveness of the power delivery from a transmission line to a load, expressed in decibel (dB).

$$RL(\text{dB}) = 10\log_{10}\left(\frac{P_{\text{in}}}{P_{\text{ref}}}\right) \quad \text{(I.8)}$$

Where p_{ref} is the reflected power and p_{in} is the input power.

In RF/microwave applications, Return loss is expressed using scattering parameter S_{11} [5]:

$$\text{RL(dB)} = -20\text{l0g}_{10}|S_{11}| \quad \text{(I.9)}$$

I.4.4 Center frequency

The center frequency (F_c) of a filter is a measure of a central frequency between the upper and lower 3 dB frequencies [6]. F_c may not necessarily be the peak transmission point of the load of the band pass filter. Usually it is defined as the arithmetic mean or geometric mean of the lower and upper cut-off frequencies,

$$\text{Arithmitic mean } = F_c = \frac{F_{-3dB_H} + F_{-3dB_L}}{2} \quad \text{(I.10)}$$

$$\text{Geometric mean } = F_c = \sqrt{\left(F_{-3dB\text{H}}\right) X \left(F_{-3dB_{\text{L}}}\right)} \quad \text{(I.11)}$$

I.4.5 Fractional bandwidth

Fractional bandwidth is the bandwidth of a device divided by its center frequency defined by:

$$FBW = \frac{BW}{F_C} \quad \text{(I.12)}$$

I.4.6 Quality factor

The quality factor (Q) of a filter is the ration of the center frequency to bandwidth. In other words, the inverse of FBW

$$Q = \frac{F_c}{BW} \quad \text{(I.13)}$$

I.4.7 Cut-off frequency

The cut-off frequency ($f_{cut\text{-}off}$) is the frequency at which the filter **IL** is equal to 3dB, or where the output power becomes only half of the input power magnitude. At this point, the attenuation amount due to the filter starts to increase rapidly.

I.4.8 Stop band

The IEEE definition of the stop band is: “the range of frequencies within which the attenuation of a filter or network is higher than at frequencies outside the range” [7]; stop band is a range of frequencies, between specified limits, at which the filter insertion loss is greater than a specified value [8]

I.5 Microstrip line transmission

I.5.1 Microstrip history

Microstrip is a planar transmission line that consists of two layers of copper separated by a lossy dielectric, it was developed by ITT laboratories by Grieg and Engelmann in December 1952 as a competitor to the stripe line, due to the fields within two guided-wave media, the Microstrip does not support a pure TEM wave which provides unpredictable results, the thin version of Microstrip became popular in 1960s.

I.5.2 Microstrip structure

Microstrip transmission lines consist of a conductive strip of width W, conductive thickness t and a ground plane, separated by a dielectric layer of thickness h and a constant relative dielectric ε_r. As shown in Figure I.6

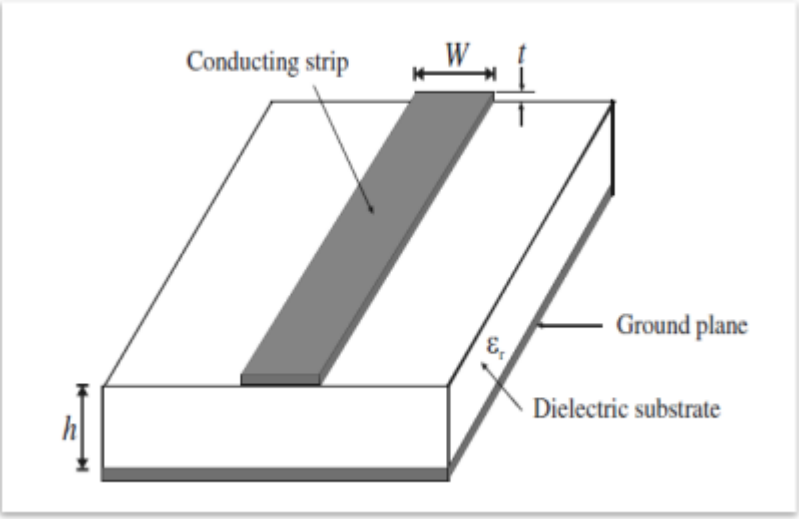

Figure I.6 Microstrip transmission line [9]

I.5.3 Analysis formulas

➢ **Effective dielectric constant**

The dielectric constant is a measure of the extent to which it concentrates electrostatic line of flux. Because of the fields from the microstrip conductor exists in the air, the effective dielectric constant (ε_{eff}) is somewhat less than the substrate's dielectric constant ε_r (also known as the relative permittivity).knowing that W is the strip width and h is the substrate thickness, the effective dielectric constant of the microstrip is calculated as follows

- When $\left(\frac{W}{h}\right) < 1$

$$\varepsilon_{eff} = \frac{\varepsilon_r+1}{2} + \frac{\varepsilon_r-1}{2}\left[\left(1+12\left(\frac{W}{h}\right)\right)^{-1/2} + 0.04\left(1-\left(\frac{W}{h}\right)\right)^2\right] \quad (I.14)$$

- When $\left(\frac{W}{h}\right) \geq 1$

$$\varepsilon_{eff} = \frac{\varepsilon_r+1}{2} + \frac{\varepsilon_r-1}{2}\left(1+12\left(\frac{W}{h}\right)\right)^{-1/2} \quad (I.15)$$

➢ **Characteristic impedance**

The characteristic impedance of the microstrip is calculated as follows [10] :

- When $\left(\frac{W}{h}\right) < 1$

$$Z_0 = \frac{60}{\sqrt{\varepsilon_{eff}}} \ln\left(8\frac{H}{W} + 0.25\frac{W}{h}\right)(Ohms) \quad (I.16)$$

- When $\left(\frac{W}{h}\right) \geq 1$

$$Z_0 = \frac{120\pi}{\sqrt{\varepsilon_{eff} \times \left[\frac{W}{h} + 1.393 + \frac{2}{3}\ln\left(\frac{W}{h} + 1.444\right)\right]}} (Ohms) \quad (I.17)$$

➢ **Guided wavelength**

Knowing that λ_0 is the wavelength in free space, the guided wavelength is given by [11]:

$$\lambda_g = \frac{\lambda_0}{\varepsilon_{eff}} \quad (I.18)$$

➢ **Propagation constant**

Propagation constant $\boldsymbol{\beta}$ is given by [5]

$$\beta = \frac{2\pi}{\lambda_g} \quad (I.19)$$

➢ **Electrical length**

For a given physical length of a microstrip l, the electrical length is

$$\theta = \beta l \quad (I.20)$$

➢ **Phase velocity**

Phase velocity v_p is given by:

$$v_p = \frac{\omega}{\beta} = \frac{c}{\sqrt{\varepsilon_{eff}}} (m/s) \quad (I.21)$$

Where c is the light velocity in free space ($c = 3 \times 10^8\, m/s$) [5]

I.6 Defected ground structure (DGS) technique

In recent years, there have been several new concepts applied to distributed microwave circuits. One such technique is defected ground structure or DGS, where the ground plane metal of a microstrip (or stripline, or coplanar waveguide) circuit is intentionally modified to enhance performance.

The name for this technique simply means that a "defect" has been placed in the ground plane, which is typically considered to be an approximation of an infinite, perfect-conducting current sink. Of course, a ground plane at microwave frequencies is far removed from the idealized behavior of perfect ground. Although the additional perturbations of DGS alter the uniformity of the ground plane, they do not render it defective [13].

First DGS proposed in 1999, later, many researchers have proposed alternate designs that have boosted the applicability of DGS. The main advantages of DGS over PBG as few DGS elements can achieve similar parameters as periodic PBG and can show the slow-wave effect [14]-[15]. As mentioned, the DGS has a defect that is etched on the uniform ground plane, which alters the uniformity of the ground plane, thus called Defected Ground Structure, this etched defect in the ground plane disturbs the shielding current distribution, which alters and rise the inductance and capacitance of the line [16], the shielding current distribution depends on the shape and dimensions of the defect and the band gap property relies on many design parameters such as lattice shape, lattice spacing, and number of lattice [15].

Another advantage of DGS is by cascading the unit cell we can achieve deeper and steeper stop band depending on the number of cells. The cascading can be in both horizontal and vertical direction, but with the conventional planar transmission line, vertical cascading is not possible. Cascading has to be done along the transmission line direction [16].

The etched section of DGS increases the series inductance which in turn increases the reactance of the microstrip with increase in frequency. This gives a start for the rejection of certain frequency range. The attenuation pole location is provided by the series inductance in parallel with the capacitance. This acts like a parallel LC resonator. The unwanted surface waves, leakage and spurious signals can be suppressed with stopband characteristics of DGS. The reactance of capacitance decreases with the increase in frequency.

DGS can provide sharp selectivity at cut-off frequency and excellent performance in terms of spurious signals in stop band and ripples in pass band [16]. Using DGS, we can suppress harmonics too. Many researchers have combined DGS with new materials to achieve special characteristics like tonality and more. In [17] a filter is designed using DGS and LTCC and moreover substrate integrated waveguide (SIW) was adopted and combined with the DGS in [18].

The LC equivalent components of DGS causes slow wave effect which is one of the most important advantages of DGS. The transmission line with DGS when compared to conventional lines has higher impedance and slow wave factor [16]. With these

properties the circuit sizes can be reduced. DGS can be applied to microwave oscillators, microwave couplers (to increase the coupling), microwave filters, microwave amplifiers etc. DGS is also used in microstrip antenna design for different applications such as antenna size reduction, cross polarization reduction and harmonic suppressions.

I.7 Defected ground structure characteristics

The basic element of DGS is a resonant gap or slot in the ground metal, placed directly under a transmission line and aligned for efficient coupling to the line. Figure I.6 shows several resonant structures that may be used. Each one differs from occupied areas, equivalent L-C ratio, coupling coefficient, higher-order responses, and other electrical parameters. A user will select the structure that works best for the particular application. The equivalent circuit for a DGS is a parallel-tuned circuit in series with the transmission line to which it is coupled as shown in figure I.8

The input and output impedances are that of the line section, while the equivalent values of L, and R are determined by the dimensions of the DGS structure and its position relative to the transmission line. The range of structures, of which figure I.7 is only a sample, arises from different requirements for bandwidth (BW) and center frequency, as well as practical concepts such as a size/shape that does not overlap other portions of the circuit, or a structure that can be easily trimmed to the desired center frequency.

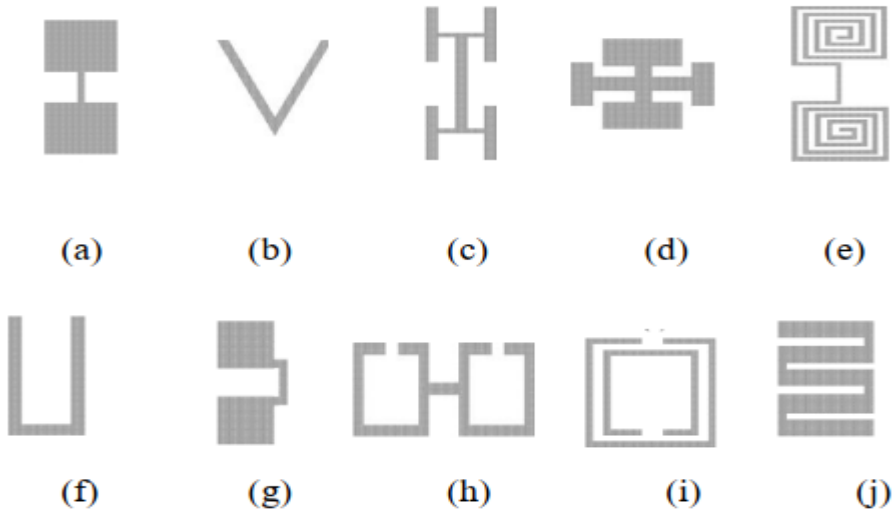

Figure I.7 different DGS geometry: (a) dumbbell-shaped (b) V-shaped (c) H-shaped (d) Cross-shaped (e) Spiral-shaped (f) U-shaped(g) square heads connected with U slots (h) open loop dumbbell (i) split-ring resonators (j) meander line [19].

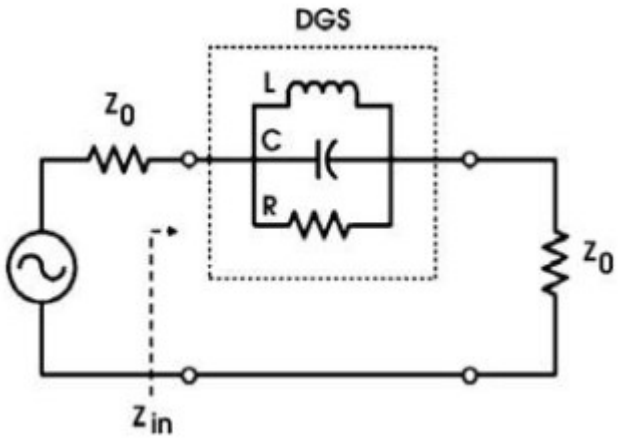

Figure I.8 Equivalent circuit of the unit DGS [20].

The values of L, C and R are determined by the dimensions and location relative to the "through" transmission line.

The values of the capacitor, the inductor and the resistance can be obtained as follows [20]:

$$C = \frac{\omega_c}{2Z_0(\omega_0^2 - \omega_c^2)} \quad (I.22)$$

$$L = \frac{1}{4\pi^2 f_0^2 C} \quad (I.23)$$

$$R = \frac{2Z_0}{\sqrt{\frac{1}{|S_{11}(\omega_0)|^2} - \left(2z_0\left(\omega_0 C - \frac{1}{W_0 L}\right)\right)^2 - 1}} \quad (I.24)$$

I.8 Applications, advantages, and disadvantages

Applications, advantages, and disadvantages of different types of DGS are summarized in table I.1 [21]

Shape	Advantages	Disadvantages	Applications
Dumbbell	Simple structure, easy to design and analyze	Single stop band	Band-stop filter
VPDGS	44.4% size reduction	Dispersion problem	Matching network of amplifier
HPDGS	38.5% size reduction	Large size than VPDGS, Dispersion problem	Matching network of amplifier
U-slot	Improved Q-factor	Single stop band	Band-stop filter
V-slot	Improved Q-factor	Single stop band	Band-stop filter
Cross DGS	Sharp rejection, Ultra wide stop band	-	Low-pass filter
Fractal DGS	Wide stop band	No sharp cut-off frequency	Band-stop filter
Spiral DGS	Multi-stop band	Complex analysis	Band-stop filter

Table I.1 Applications, advantages, and disadvantages of different types of DGS [21]

I.9 DGS effects in microwave circuit

There are widely applications in active and passive devices useful for compact design. Since each DGS provides its own distinctive characteristics depending on the geometries, such circuit functionalities as filtering unwanted signals and tuning high-order harmonics can easily be accomplished by means of placing required DGS patterns, which correspond to the desired circuit operations without increasing circuit complexity.

- **Stop Band effect**

DGS, which is realized by etching off a defected pattern or periodic structures from the backside metallic ground plane, has been known as providing rejection of certain frequency band, namely, bandgap effects. The stopband is useful to suppress the unwanted surface

waves, spurious and leakage transmission. Therefore, a direct application of such frequency selective characteristics in microwave filters is becoming a hotspot research recently.

DGS provides excellent performances in terms of ripples in the passband, sharp-selectivity at the cut-off frequency and spurious free wide stopband. There have two types of filter design using DGS: one is directly using the frequency-selectivity chrematistic of DGS to design filters [22–23], the other is using DGS on the conventional microstrip filters so as to improve performance [24–25].

- **High Characteristic Impedance**

It is a serious problem for the conventional microstrip line case that the generally accepted impedance is limited to realize is around 100 ~ 130 Ω. By adopting DGS on the ground plane is possible to increase the equivalent inductance *L* highly, and to decrease the equivalent *C* at the same time, and finally to raise the impedance of the microstrip line more than 200 Ω.

I.10 Conclusion

In several areas of RF/microwave engineering, filter networks are critical building blocks. In a variety of RF/microwave systems and equipment, such networks are used to select/reject or separate/combine signals at different frequencies. The structure of the circuit network is the same for all, while the physical realization of filters at RF/microwave frequencies varies [26].

Microstrip filters are used to confine microwave signals within specified spectral limits. The use of DGS units in the metallic ground plane of a microstrip line is an appealing approach for achieving slow-wave characteristics and a rejection band when the shield current distribution in the ground plane is disrupted or perturbed [27].

UWB filters are essential components in a wide range of current applications. To fulfil the required UWB frequency mask (3.1 to 10.6 GHz), a UWB BPF with low IL and good out-of-band rejection is preferred [27] [28].

CHAPTER II

UWB TECHNOLOGY AND FILTERS

II.1 Introduction

The need for wireless wideband communications is quickly expanding due to the requirement to accommodate a bigger number of users and provide more information at higher data rates. The use of UWB technology could be a solution. This latter is currently attracting a lot of interest since it provides wireless communications' simplicity and mobility to high-speed interconnects in devices throughout the digital home and office. [29]. This innovation takes a completely new approach to wireless communication. [30].

II.2 Historical perspective

UWB communication is not a new technology. It was first employed by G. Marconi in 1901 to transmit Morse code sequences across the Atlantic Ocean using spark gap radio transmitters. However, the benefit of a large bandwidth and the capability of implementing multi-user systems provided by electromagnetic pulses were never considered at that time.

Approximately 50 years after G. Marconi, modern pulse-based transmission gained momentum in military applications in the form of impulse radars. The genesis of UWB technology is a result of the research works in time-domain electromagnetic that began in 1962. The concept was to characterize linear, time-invariant (LTI) systems by their output response (i.e., amplitude and phase measurement of impulse excitation and measurement techniques. Once these techniques were in place, it became obvious that they could be used for short pulse radar and communication systems.

Many of the communication technologies were first experimented and used in military applications for some decades, only to be used for commercial applications at a much later time. UWB is no exception to this trend. From the 1960s to the 1990s, this technology was restricted to military and Department of Defense (DoD) applications under classified programs such as highly secure communications. In 1978, G.F. Ross and C.L. Bennet applied these techniques for radar and communication applications. This technology was referred to

as base-band, carrier-free, or impulse until the late 1980s and was termed UWB by the U.S. DoD around 1989. By that time, UWB theory had experienced 30 years of development [31]

Although UWB technology is old, its application for communication is relatively new. The recent advancements in microprocessor and fast switching in semiconductor technology has made UWB ready for commercial applications. Therefore, it is more appropriate to consider UWB as a new name for a long-existing technology. As interest in the commercialization of UWB has increased over the past several years, developers of UWB systems began pressuring the FCC to approve UWB for commercial use.

II.3 Definition

UWB is a wireless technology for transmitting huge amounts of digital data over a wide spectrum of frequency bands with very low power for a short distance.

UWB radio not only can carry a huge amount of data over a distance up to 230 feet at very low power (less than 0.5mW), but has the ability to carry signals through doors and other obstacles that tend to reflect signals at more limited bandwidths and higher power(penetration). It broadcasts digital pulses that are timed very precisely on a carrier signal across a very wide spectrum (number of frequency channels) at the same time. Transmitter and receiver must be coordinated to send and receive pulses with an accuracy of trillionths of a second [31].

This technology modulates impulse based waveforms instead of continuous carrier waveforms. As explained above, the principles of UWB are extremely short pulses; and very low duty cycles at time domain. For frequency domain, ultra-wide spectrum, low power spectral density, and acceptable interference with other users are main principles. It enables spectrum reuse as 3.1-10.6 GHz to coexist with other users. The multipath immunity is in the form that path delay is much greater than pulse width. UWB signaling has many attributes that make it attractive for a wide range of applications; from wireless sensors to streaming wireless multimedia and wireless USB….etc [33] [32].

II.4 UWB technology advantages

The UWB impulse radio system does have several advantages over other conventional systems [34].

1. **High data rate wireless transmission:**

Due to the ultra-wide bandwidth of several GHz, UWB systems can support more than 500 Mb/s data transmission rate within the range of 10 m, which enables various new services and applications.

2. **High precision ranging:**

   Due to the nanosecond duration of typical UWB pulses, UWB systems have a good time-domain resolution and can provide centimeter accuracy for location and tracking applications.

3. **Low loss penetration:**

   UWB systems can penetrate obstacles and thus operate under both line-of-sight (LOS) and non-line-of-sight (NLOS) environments.

4. **Fading robustness:**

   UWB systems are immune to multipath fading and capable of resolving multipath components even in dense multipath environments. The transceiver complexity can be reduced by taking the advantages of the fading robustness. The resolvable paths can be combined to enhance system performance.

5. **Security:**

   For UWB signal, the power spectral density is very low. Since UWB systems operate below the noise floor, it is extremely difficult for unintended users to detect UWB signals. The probability of intercept is low in UWB. The UWB system is also difficult to be interfered with because of its huge bandwidth.

6. **Coexistence:**

   The unique character of low power spectral density allows UWB system to coexist with other services such as cellular systems, wireless local area networks (WLAN), global positioning systems (GPS), etc.

7. **Low cost transceiver implementation:**

   Because of the low power of UWB signals, the RF chip and baseband chip can be integrated into a single chip using CMOS technology. The up-converter, downconverter, and power amplifier commonly used in a narrowband system are not necessary for UWB systems. The UWB can provide a low cost transceiver solution for high data rate transmission. UWB systems communicate by modulating a train of pulses instead of a carrier. The carrier-less nature of UWB results in simple, low power transceiver circuitry, which does not require intermediate mixers and oscillators.

These benefits allow the UWB radio to become a very attractive solution for future wireless communications and many other applications including logistics, security applications, medical applications, control of home appliances, search-and-rescue, supervision of children, and military applications [35].

II.5 UWB technology disadvantages

Here are some of the disadvantages of this technology [31]:

1. **Interference:** Interference is one of the major challenges in the design of UWB communication systems. Since UWB communication devices occupy a large frequency spectrum. Interference avoidance with coexisting users is one of the key issues of UWB technology. Existing electronic devices include current IEEE 802.11a WLAN devices (working at 5.150-5.825 GHz) and 2. GHz industrial, scientific, and medical (ISM) band devices, that are used by wireless personal area networks like Bluetooth.
2. **Complex signal processing:** For narrowband systems that use carrier frequency, frequency-division; multiplexing is very straightforward and the development of a narrowband device needs to consider the frequency bands directly affecting it and filtering and wave shaping. For carrier-less transmission and reception, every narrowband signal in the vicinity is a potential interfere and also every other carrier-less system. So, any carrier-less system has to rely on relatively complex and sophisticated signal processing techniques to recover data from the noisy environment.
3. **Bit Synchronization time:** since pulses with picosecond precision are used in UWB, the time for a transmitter and receiver to achieve bit synchronization can be as high as a few milliseconds. So, the channel acquisition time is very high, which can significantly affect performance, especially for intermittent communications.
4. **Short range area:** information can travel only for short distances (10-20m) due to low power transmission.

II.6 UWB technology applications

In radars

- Vehicular radars used for collision detection/avoidance and sensing road conditions.
- Ground penetrating radars.
- Tags identification.
- Through wall imaging used rescue, security and medical applications.

In wireless communications systems

- Transferring large amounts of data using wireless networks in short-range for home or office networking.
- Short range voice, data, and video applications (a television set and computer system without wires and transferring data at a higher rate than wired connections).
- Military communications, on board helicopters and aircrafts that would otherwise have too many interfering multipath components.
- Roadside information that can be deployed where the messages may contain weather reports, road conditions, construction information and emergency assistance communication.

In localization and tracking

- Accurately locating a person or object within one inch of its location through any structure; Global positioning system (GPS) technology is only accurate up to 1m and does not work inside buildings; GPS is expensive but UWB will be low cost.
- Detecting land mines.
- Assessing enemy locations and tracking troops.
- Localization in search and rescue efforts, tracking of livestock and pets.

II.7 Development of UWB Bandpass Filters

After the release of UWB, bandpass filters with a passband of the same frequency range (3.1 GHz – 10.6 GHz, a fractional bandwidth of 110%) were challenged for conventional filter designs. Before mid 2003, the bandwidth of the passband for bandpass filters was extended from 40% to 70%. These filters are named broad bandpass filters. They were not covering the whole UWB frequency range yet. A bandpass filter covering the whole UWB frequency range with a fractional bandwidth of 110% was realized by fabrication signal lines on a lossy composite substrate. The main problem of the early reported filters that possess an ultra-wide passband was their high insertion loss in the passband due to the lossy substrate. Not much research work was reported in 2003 and 2004. In 2004, a ring resonator with a stub was proposed which shows a bandwidth of 86.6%. A bandpass filter covering the whole UWB frequency band was a challenge for microwave filter designers and researchers in that period of time.

In 2005, there were 11 conference papers in total published in International Microwave Symposium, International conference on Ultra-Wideband, Asia-Pacific Microwave Conference, or European Microwave conference. In the same year, there were four journal publications. There are mainly four types of structures that are able to realize an

ultra-wide -passband. One is microstrip structure shown in figure II.1. It consists of a microstrip multi-mode resonator (MMR) and a parallel-coupled line at each end of the network. The MMR has two identical high-impedance sections with a length of quarter guided wavelength at two sides and a low-impedance section with a length of half guided wavelength in the middle. The MMR in the filter generates first and third resonant mode at the edges of the UWB passband. The parallel-coupled lines are modified to obtain the ultra-wide passband. The second type is a hybrid coplanar waveguide (CPW) and microstrip structure. This type of structure consists of a CPW MMR on one side and a microstrip input and output on the other side, figure II.2 shows the CPW MMR. The third type of filter which is also able to have a fractional bandwidth of 110% is the broadside-coupled microstrip-CPW structure shown in figure II.3. There is a broadside-coupled microstrip line on one side of the substrate and an open-end CPW on the other side of the substrate. The last type of filters that has a bandwidth as high as around 100% is the combination of a high pass filter and a low pass filter.

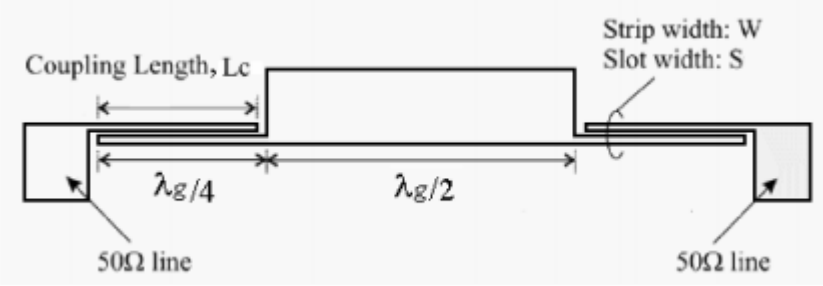

Figure II.1 the schematic of a microstrip multi-mode resonator (MMR) and two parallel coupled lines

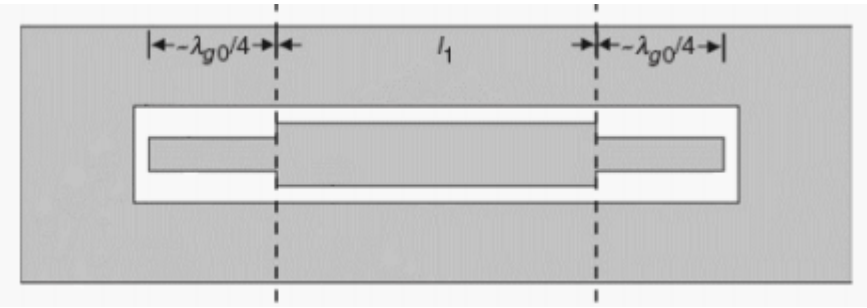

Figure II.2 the schematic of a CPW MMR

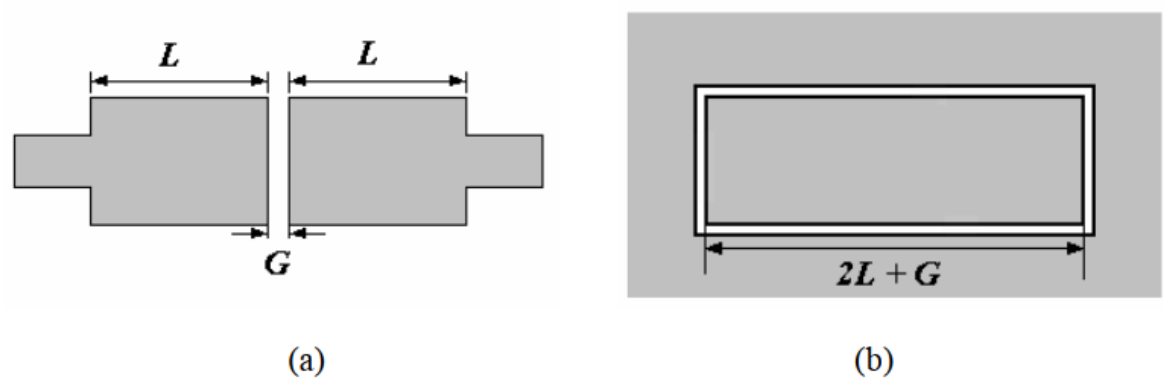

Figure II.3 the schematic of the broadside-coupled microstrip-CPW structure

(a) top view (b) bottom view

After that, these filters were further optimized with improvement in the rejection of the upper stopband. With novel high pass and lowpass structures, the bandpass filter obtained a wider bandwidth. With regards to the UWB bandpass filter designs by cascading a high pass and low pass filter, a systematic consistent and analytical method is proposed. There are a good number of new structures proposed that exhibit an ultra-wide passband. With the introduction of lumped components to a microstrip line, a miniaturized UWB BPF with a length of 0.18λg is realized. The small physical size is attributed to the lumped components used.

UWB bandpass filters with a notch stopband from 5 GHz to 6 GHz for filtering the wireless local-area network (WLAN) is proposed then, additional components are introduced providing the notch stopband at the desired frequency in addition to stopband sharpness [35].

II.8 Conclusion

The rapid development of a variety of wireless communication systems necessitated the creation of a technology that included multiple wireless communication standards. Since ultra-wideband (UWB) technologies offer advantages in terms of vast bandwidth and high-speed transmission, the use of UWB bandpass filters has received a lot of attention and several conventional methods to achieve UWB bandpass filters with desired transmission performance.

The UWB bandpass filters, as a major component of UWB technology, can be implemented utilizing a variety of dependable design approaches that produce an outstanding frequency response, which is important for scientific research and engineering.

CHAPTER III

DESIGN OF UWB BAND PASS FILTER WITH MULTIPLE NOTCHES

III.1 Introduction

In this chapter, a miniaturized ultra-wideband (UWB) band pass filter (BPF) with and without multiple notches is designed. The proposed filter occupies a surface of 30x15mm^2 on the ROGERS 4003C substrate characterized by a thickness of 0.813mm, a dielectric constant of 3.38 and a tangent loss of 0.0027.

Initially, the basic topology of our UWB filter is developed using a modified dumbbell shaped DGS; the filter has pass band from 2.7 GHz to 10.4 GHz. Later, multiple split ring resonators (SRRs) and square loop are embedded in the UWB filter to introduce the triple notches at 5.2GHz, 5.8GHz and 7.2GHz for WLAN and C band satellite applications. Simulation is carried using CST microwave studio software where fabrication and measurement are made using MITS Electronics and ROHDE & SCHWARZ vector network analyzer (VNA) respectively.

III.2 Design procedures for BPF

III.2.1 Proposed UWB-BPF

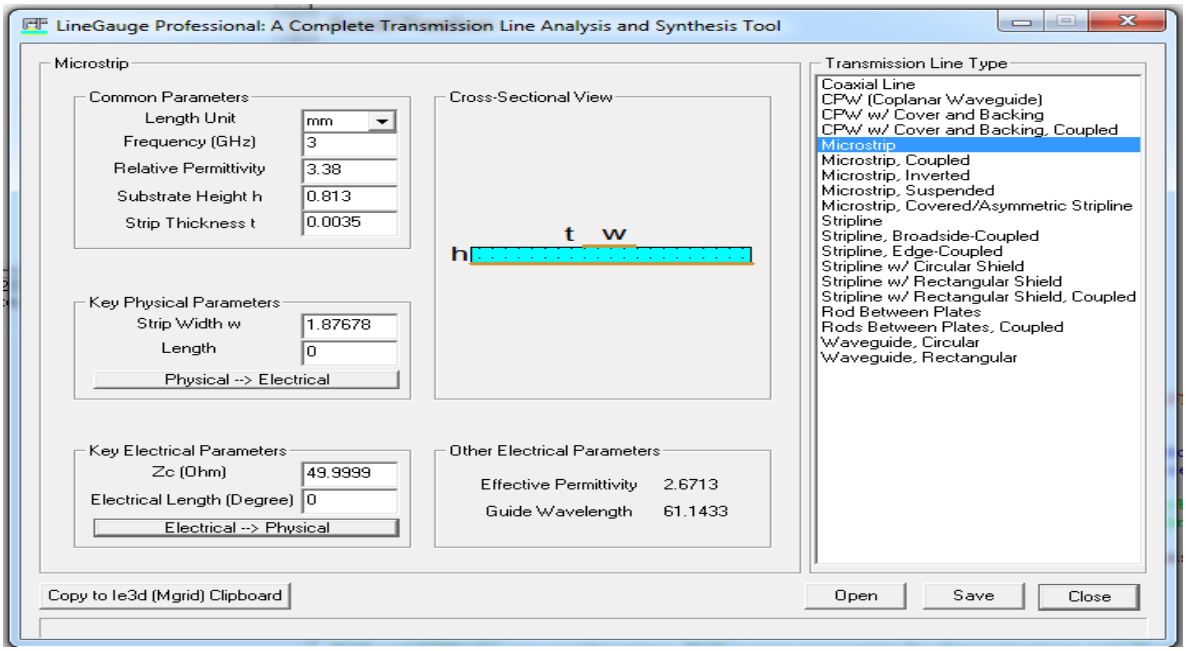

Figure III.1 LineGauge tool

We start the design by calculating the strip-line width that leads to a line impedance Z0= 50ohm, by using LineGauge tool integrated with IE3D software as depicted in Figure III.1

In the next step, we propose our initial design shown in Figure III.2(a-b), which consists of modified dumbbell shaped DGS on the ground plane alongside with E shaped microstrip line. The design is characterized by the parameters L, T0, W, L2, and H for the top. In addition to L3, T1, D, G1, G2 and H2 for the ground plane. Table III.1 lists the initial structure dimensions while the simulated S parameters are demonstrated in Figure III.3

Table III.1 initial dimensions of the proposed structure

Parameter	L	T0	W	L2	H	L3	T1	D	G1	G2	H2
Dimension (mm)	11.8	1	1.88	5.55	9.8	15.5	1.14	4.5	1	1.5	3.1

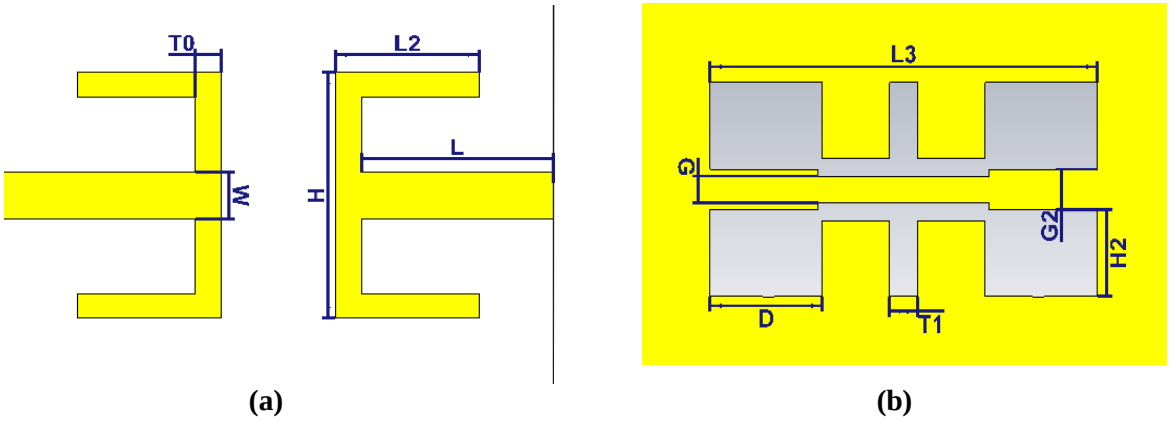

(a) **(b)**

Figure III.2 (a) Top view (b) Bottom view

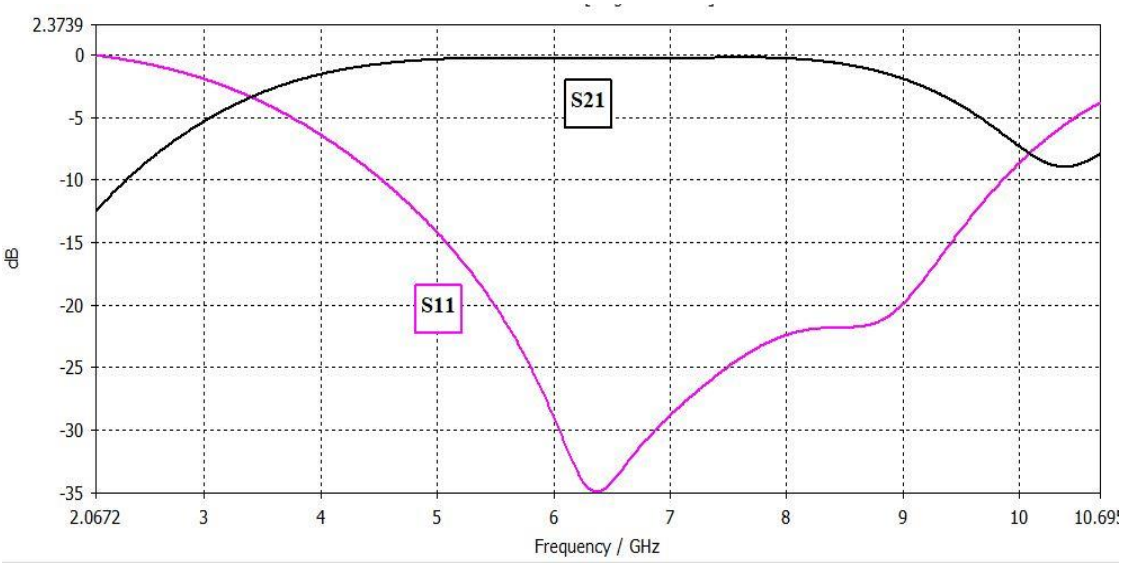

Figure III.3 magnitude of S parameters for the proposed design

From Figure III.3, it can be seen that the structure satisfies the general behavior of a band pass filter. However, the results are unacceptable in terms of bandwidth required for the ultra-wide band since the -10dB bandwidth for S11 is only around 5.3GHz (4.5GHz – 9.8GHz). In order to enhance the design performance, a parametric analysis is performed to investigate the influence of different geometric parameters on the results and pick the most suitable for our application.

III.2.2Parametric analysis

The goal of this part is to get the best possible response of S11 and S21 by selecting the most appropriate values for the structure parameters. We start by sweeping L from 3 mm up to 5 mm in five steps so that the length of the microstrip line varies between 10 mm and 12 mm, which leads to the results shown of Figure III.4.

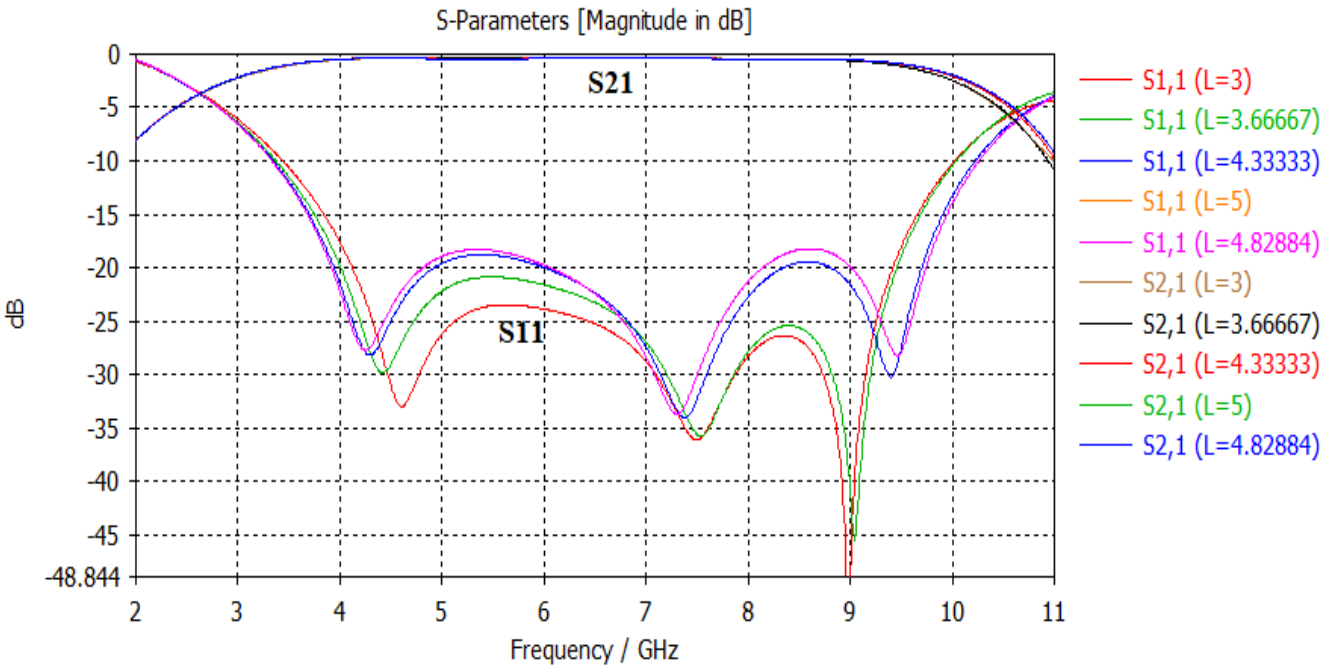

Figure III.4 simulated response of S11 and S21 for different L values

From the above graph, it is clear that the change of L does not affect S21 that much. Unlike S11 that changed between good magnitude response for the case of L=3, and a good bandwidth response as shown for L=4.82, which gives the best result in terms of -10dB bandwidth, accompanied with an acceptable magnitude response throughout the entire band which makes it suitable for the design.

The next step is to choose the best copper line width that leads to a better performance. Figure III.5 shows the variation of S parameters due to the change of T0 between 0.6 mm and 1.2 mm

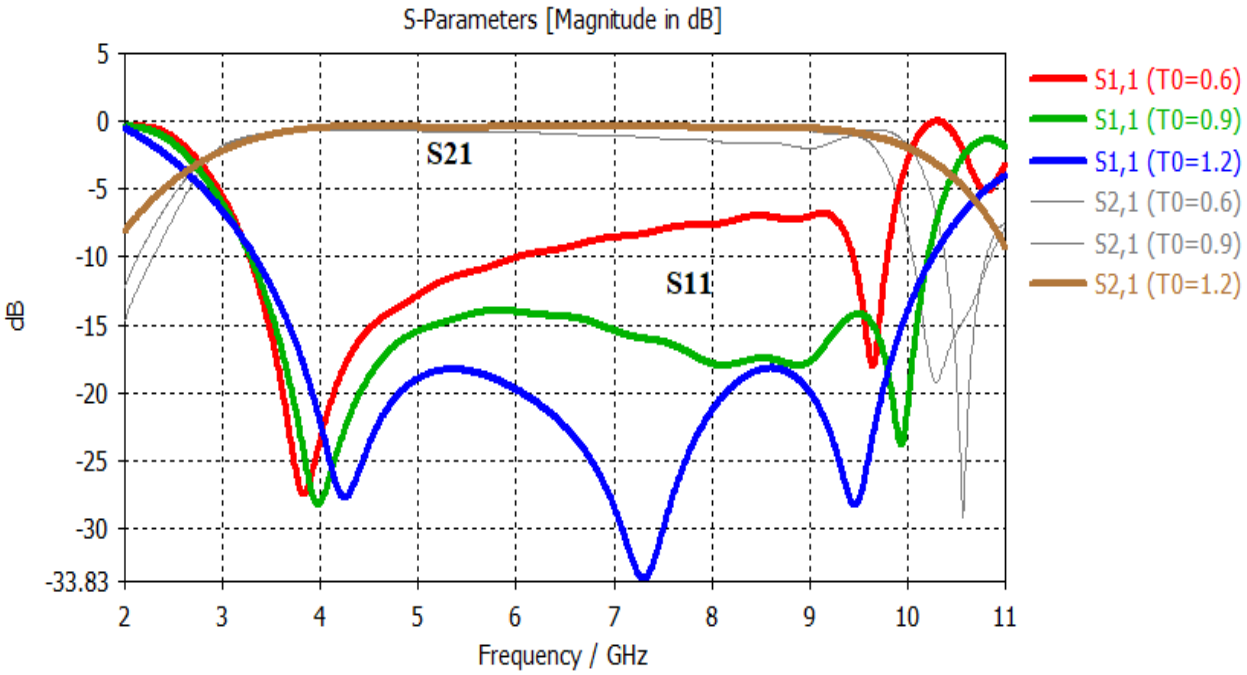

Figure III.5 S parameters change due to T0 variation

The results display the high sensitivity of the structure to the change in T0, where we can observe clear deterioration for both T0= 0.6 mm and T0= 0.9 mm. Dissimilar to T0= 1.2 mm that leads to the best response for both parameters in terms of bandwidth and magnitude. Therefore T0= 1.2mm is selected for the optimized design.

The last parameter to investigate for the top side of our structure is L2 after fixing L1 and T0 to their best possible values. Figure III.6 displays the reaction of the structure to the variation of L2.

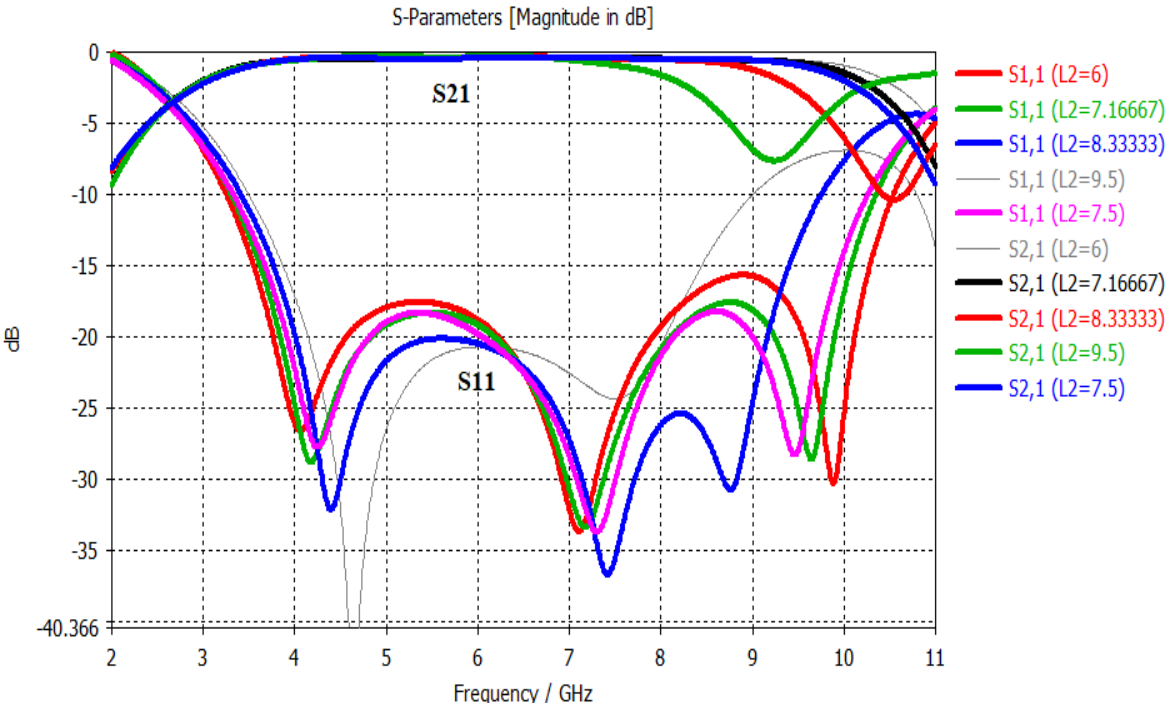

Figure III.6 S parameters change due to L2 variation

Since we have two parameters to establish, we have to select the appropriate L2 value that works best for both at the same time. As illustrated in Figure 3.6, an unacceptable value of S11 and S21 are obtained for L2= 8.33 mm and L2= 9.5 mm. Therefore, we are left with three values that lead approximately to the same bandwidth and L2= 7.5 mm is chosen to be the most suitable value as it matches the requirements.

Another critical factor is the ground geometry; it has a great influence on the design and needs to be investigated to get the most out of our design, starting with dumbbell dimensions shown in Figure III.7 alongside with S parameters values for each case

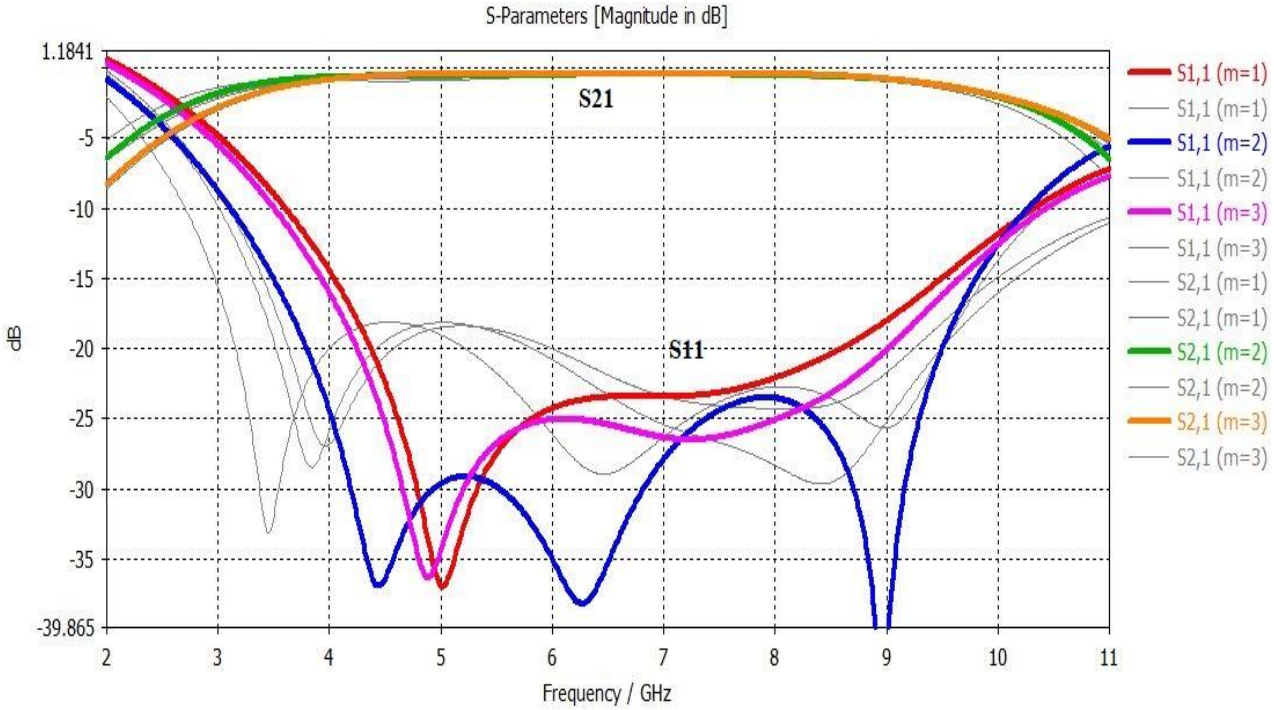

Figure III.7 parametric study of dumbbell dimensions

In this case, we have two variables sweeping at the same time and we aim to pick the pair that performs the best. As can be seen on Figure III.7, most of S11 plots do not provide the required -10 dB bandwidth, or does not even re-intersect with S21 at the end of the band. Except for the blue one which results in the desired bandwidth and magnitude, where S21 is almost unaffected by the sweep. For that reason, the values m=2 and n=1 is chosen for H2 and D respectively.

As a last step of this study, we want to vary the dimensions of the dumbbell's mid-slot to investigate its effect on S parameters response, and establish the final optimized structure that achieves the ultra-wideband BPF characteristics as the first aim of our project. Figure III.8 represents different plots of S parameters due to the variation of slot dimensions.

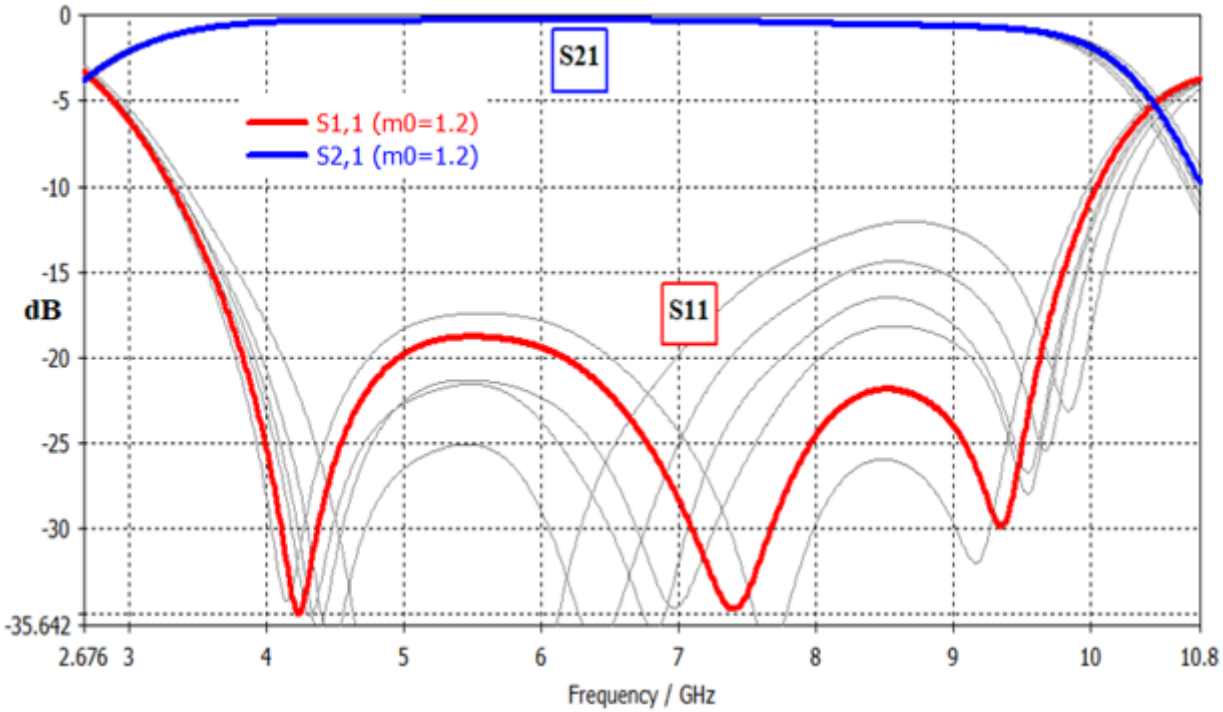

Figure III.8 parametric study of dumbbell dimensions

As Figure III.8 shows, most of S11 plots satisfy the bandwidth and magnitude standards while S21 still almost unaffected. Therefore, we end up choosing the pair m0= 1.2 and n0=1 for length and width of the slot respectively, as it provides a -10 dB bandwidth of around 7GHz (3.1 up to 10 GHz) and S parameters intersection at 10.5 GHz which is reasonable for a UWB range and leads us to the final design.

III.2.3 The final design for UWB BPF

During this part, we introduce our final design shown in Figure III.9(a-b). It basically consists of the same ground structure enhanced geometrically. However, the E shaped microstrip line is transformed into a flipped H shape on both sides due to the sensitive role of the variable L2 for a good S21 response as discussed above. The structure is defined by the parameters L, T0, W, L2, and H for the upper layer. In addition to L3, T1, D, G1, G2, G3 and H2 for the ground plane. Table III.2 lists the final dimensions while the simulated S parameters are illustrated in Figure III.10

Table III.2 Final dimensions of the proposed structure

Parameter	L	T0	W	L2	H	L3	T1	D	G1	G2	G3	H2	H3
Dimension (mm)	10.18	1.40	1.88	6.5	9.5	19.5	2.4	6.5	1	1.5	2.35	13	3.85

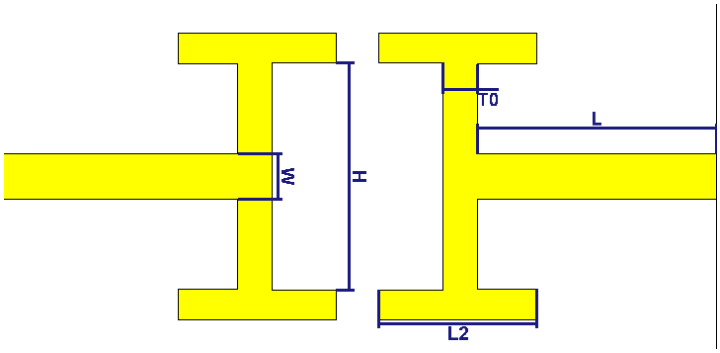

(a)

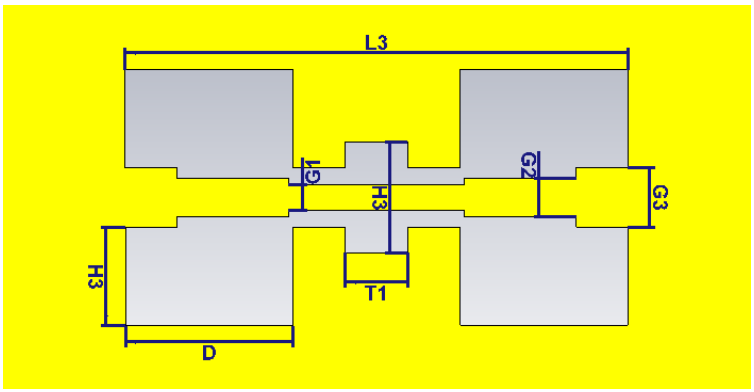

b)

Figure III.9 (a) Top view (b) Bottom view

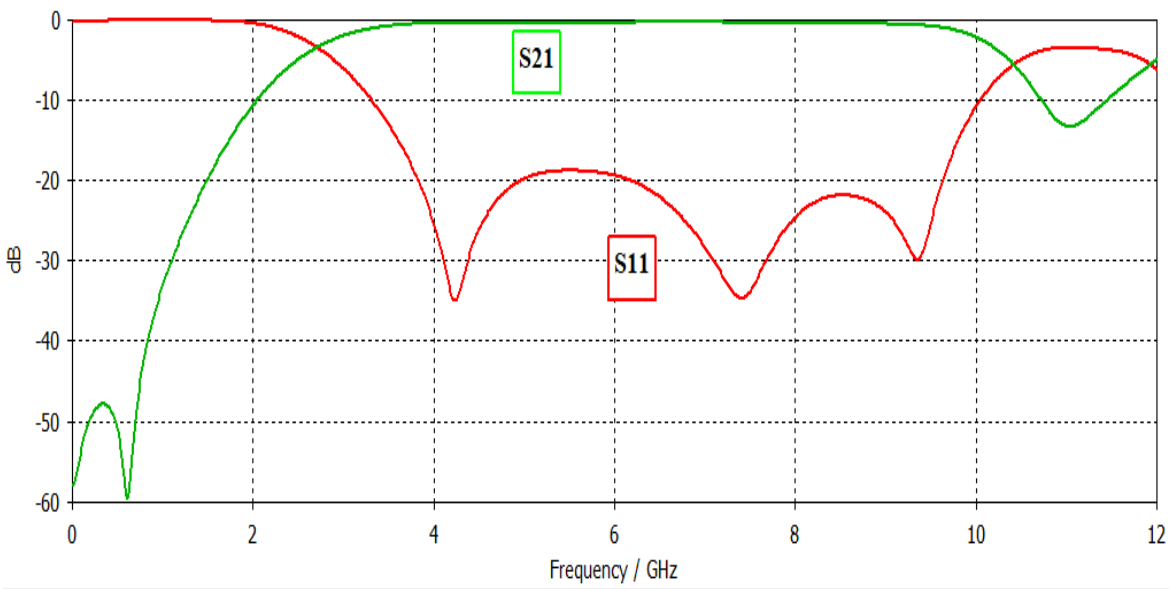

Figure III.10 magnitude of S parameters for the final design

The above figure shows the response of the final design simulated in the range 0 to 12 GHz; the filter presents a maximum flat response for the insertion loss (S21) through the entire pass

band. In addition to a return loss magnitude under -10 dB for the same frequency range alongside with a good attenuation for the stop band.

In the last step, we are going to investigate the current distribution around the structure for a pass band frequency of 6.5GHz and two stop band frequencies of 1.5GHz and 11GHz. Results from the simulated structure are shown in Figure III.11

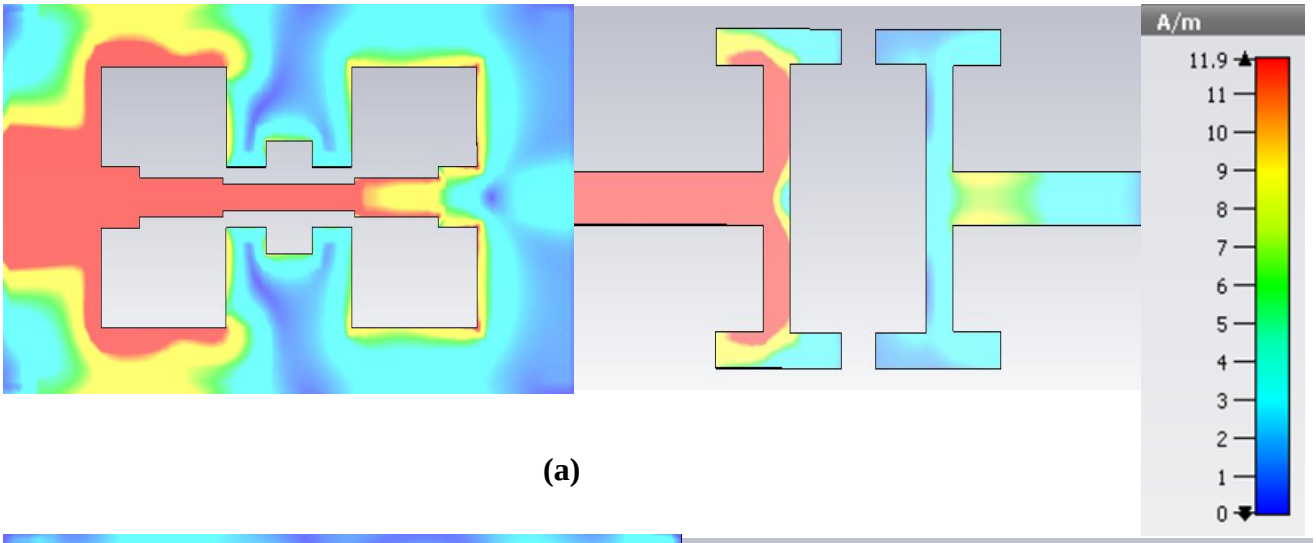

(a)

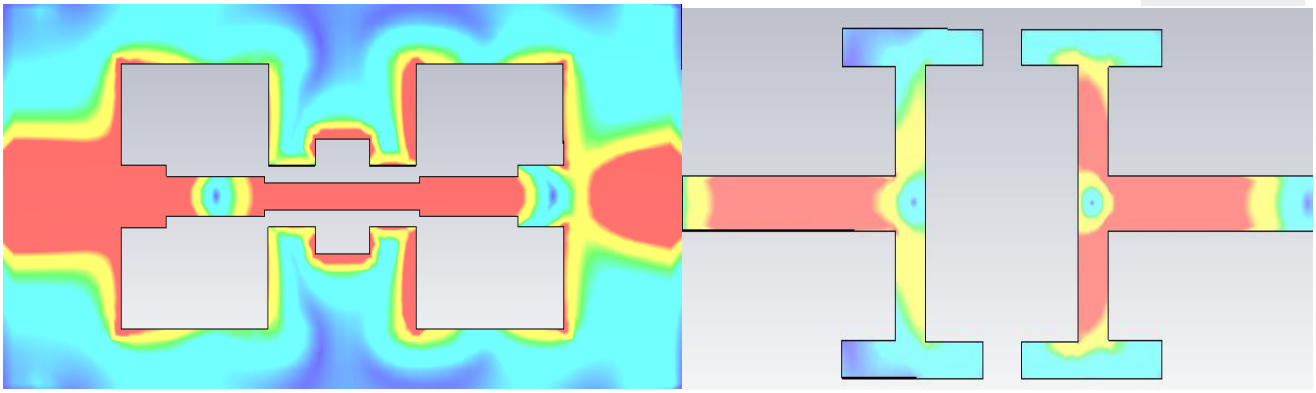

(b)

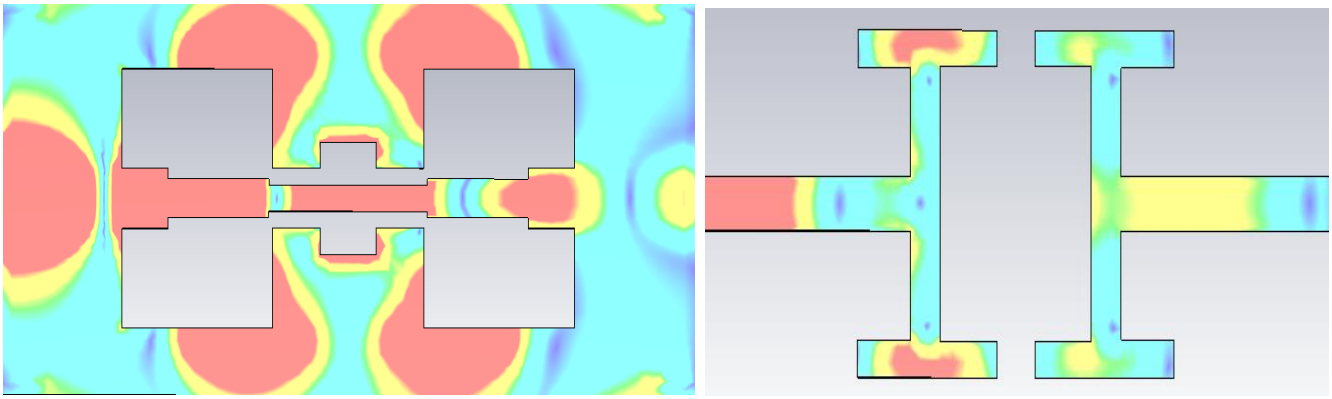

(C)

Figure III.11 current distribution at (a) 1.5GHz (b) 6.5GHz and (c) 11GHz for UWB BPF

From figure III.11 we can see how current is distributed through the entire structure of the input port until the output port, which stands for the pass band. Unlike the two stop band frequencies where the current is concentrated on the input side and gets attenuated at the output. In addition, the more we go far from the cutoff frequencies, the current gets more attenuated at the output port.

III.3 UWB BPF with multiple notches

III.3.1 single notch

For this part, the goal is to modify the structure of the filter to reject signals known to interfere with UWB signals. The selected technique is based on inserting a pair of split ring resonators (SRR) beside the feed line, without any geometrical modification of this latter. So that a notched band is created to eliminate interference with undesired WLAN signals around 5.2 GHz. The SRR pair is placed at distance 0.40 mm from the feeding line and is characterized by the shape and dimensions demonstrated by table III.3 alongside with Figure III.12.

Table III.3 dimensions of left SRR pair

Parameter	A	B	C	D	E	F	G	H
Dimension(mm)	4.30	3.2	0.52	0.30	0.37	1.80	0.4	1.72

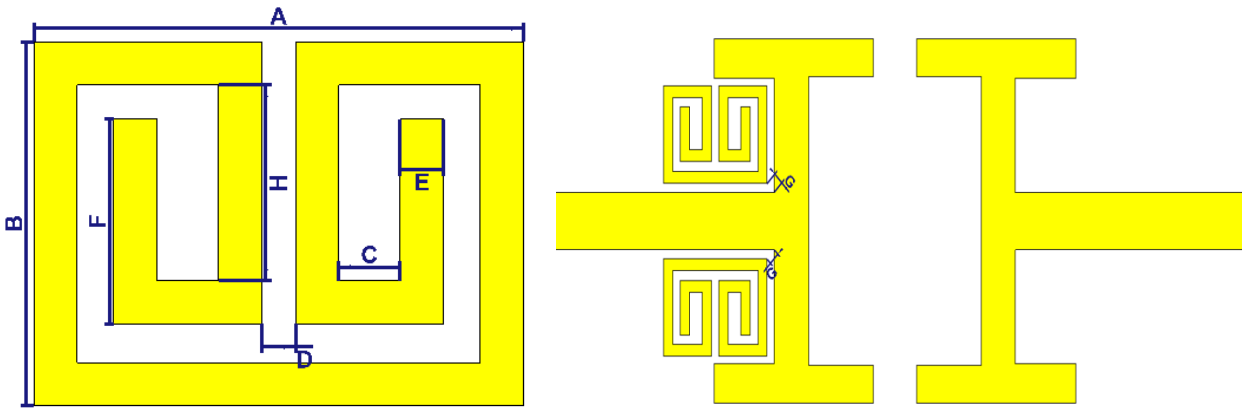

(a) (b)

Figure III.12 (a) left SRR geometry, (b) left SRR positioning

Next, we have to discuss the proposed design from a performance point of view, especially in terms of insertion loss and return loss around the notch. An insertion loss (S21) having a

magnitude lower than -10 dB is said to be acceptable. At that level, more than 90% of the incident power is attenuated. Additionally, the return loss (S11) should be as close to 0dB as possible and a value of -1dB is considered as agreeable where more than 79% of the input power is reflected. Based on these criteria and figure III.13 below that shows the simulated S-parameters response of the notched filter we are going to judge its performance.

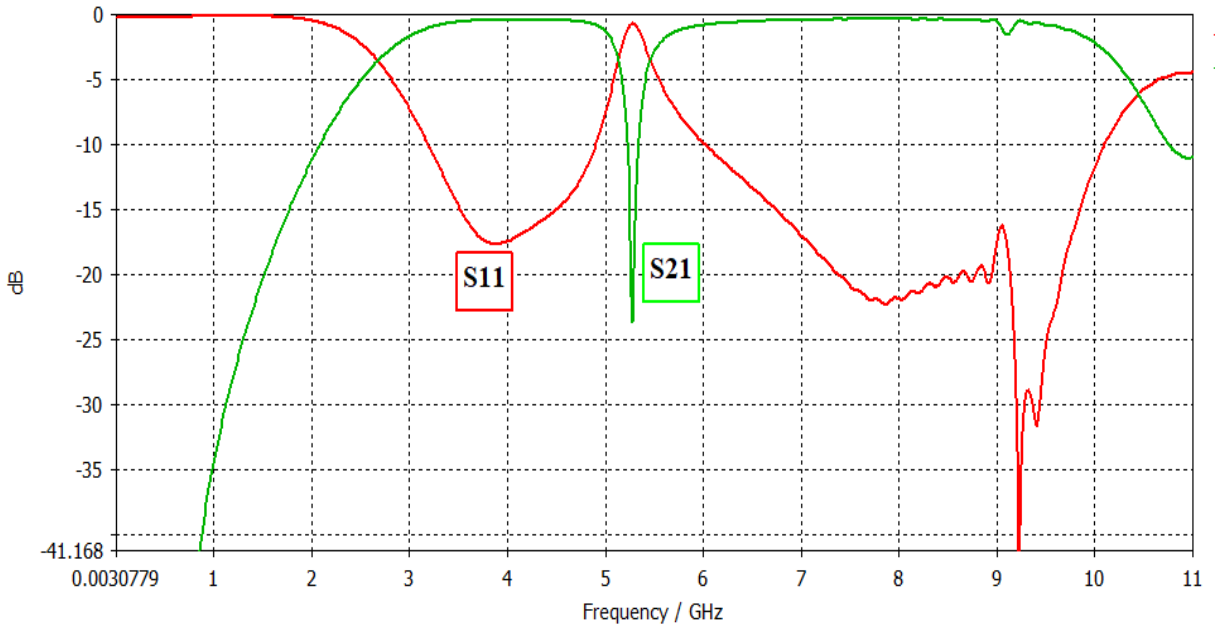

Figure III.13 S parameters response of single notched UWB BPF

As Figure III.13 shows, the notch is centered at f0= 5.2 GHz and has -3dB bandwidth of 0.35 GHz ranging between 5.03 GHz and 5.38 GHz. It presents a magnitude response approaching -25dB in terms of insertion loss, associated with a -0.6dB for the return loss which corresponds well to the criteria discussed before. In addition, the notch is surrounded with a flat passband having an insertion loss of around -0.5dB with a fluctuating return loss under -15dB, which makes the filter sharply selective and suitable for 5GHz WLAN signals rejection as will be seen on the current distribution of Figure III.14.

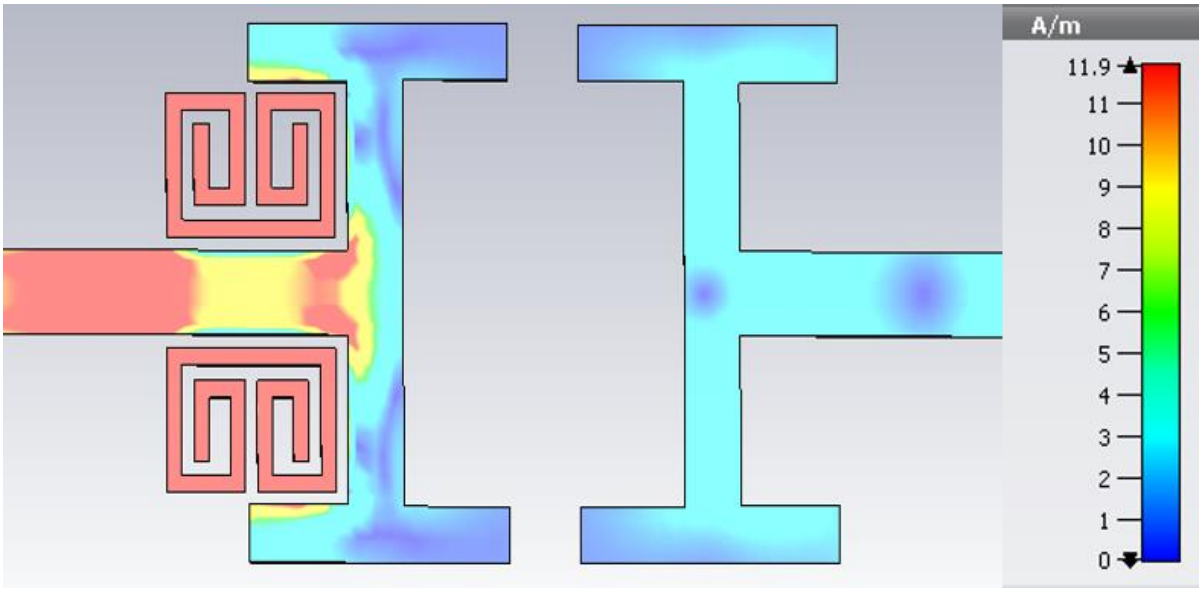

Figure III.14 current distribution at 5.2GHz

Figure III.14 demonstrates the current distribution around the structure where it is clearly seen that most of the current is concentrated at the notch, coming from the input port. However, the right side of the filter does not carry any current to the output port, which agrees totally with the results considered previously.

III.3.2 Notch parametric analysis

As notches are fundamental part of this work, we need to check the effect of different parameters on their behavior, in order to select the ones that meet the requirements. Starting by the copper thickness indicated by (E) in Figure III.12 (a). The plot below shows the high sensitivity of notch frequency to the copper thickness, where the central frequency is inversely proportional to the thickness. In addition, a change of 0.1mm is able to shift the frequency up to 0.8GHz which will be challenging in the fabrication process. Unlike the central frequency, the magnitude or the rejection level is almost unaffected.

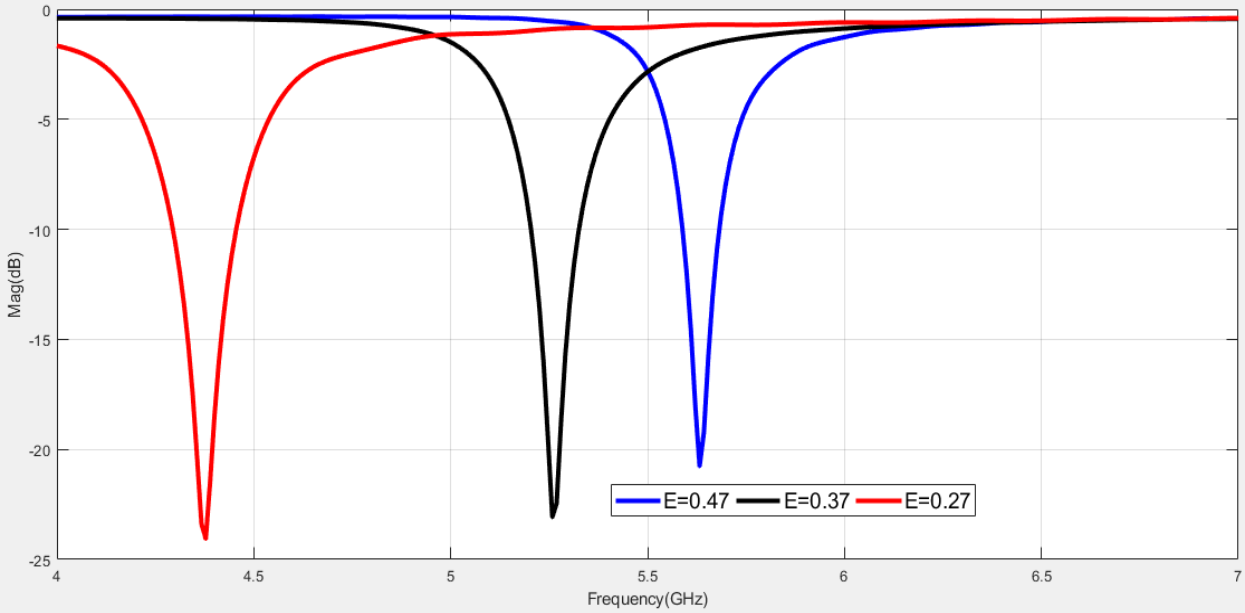

Figure III.15 The effect of copper width on notch frequency

The next step is to investigate the effect of length (F) on the response, which is shown bellow

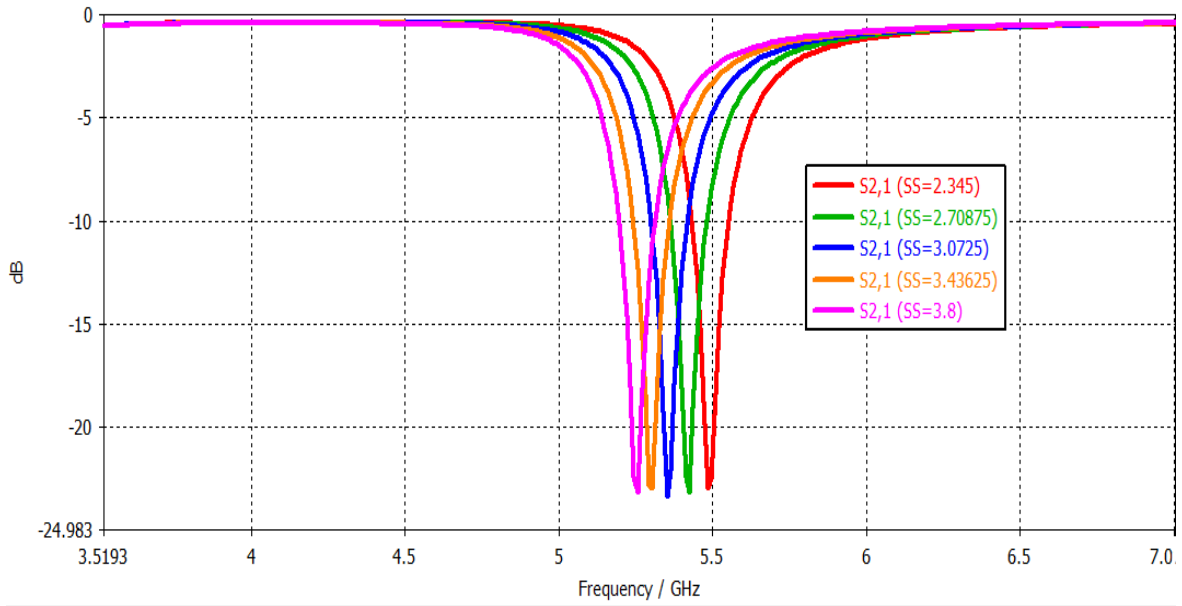

Figure III.16 notch response for different values of (F)

Figure III.16 displays different notch responses due to the change of length (F) from zero to 1.5mm where the rejection level is again unaffected that much in addition to small frequency shift inversely proportional to the length (F).

Another critical parameter to be carefully selected is the length (c). As shown on Figure III.17, the notch bandwidth is kept the same, similar to the previously discussed cases. However, the central frequency is noticeably affected by shifting up when (c) is decreased and vice versa associated with a small change in the rejection level.

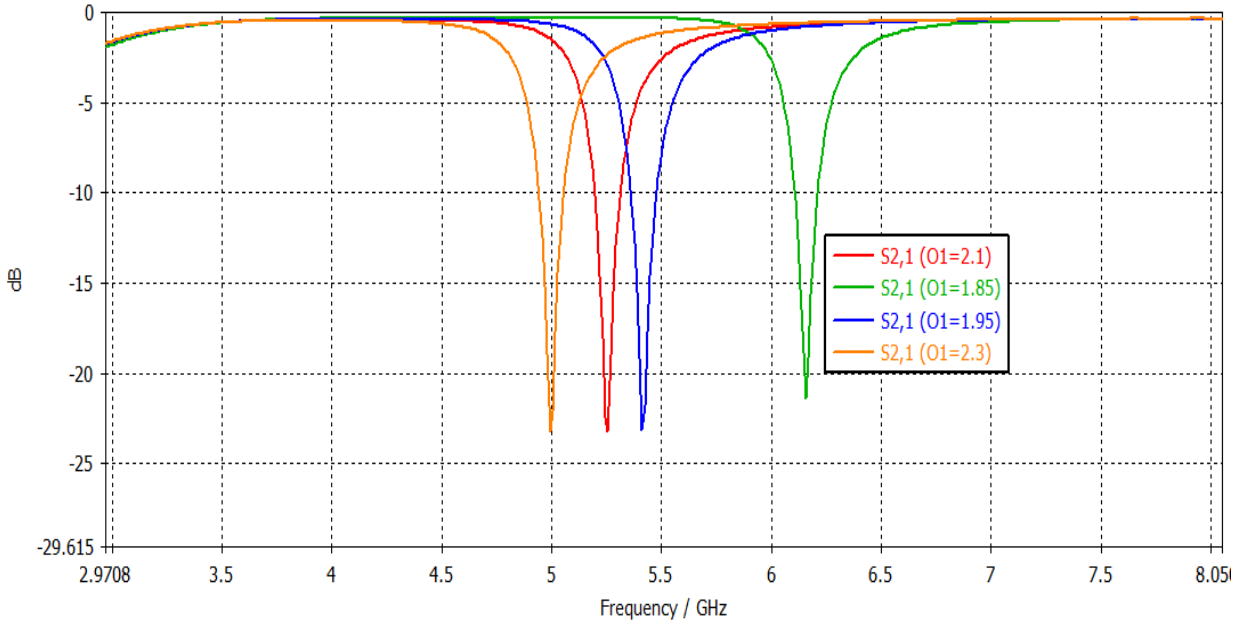

Figure III.17 notch central frequency for different values of (C)

III.3.3 Dual notched

So far, we successfully implemented a single notched UWB BPF to eliminate WLAN signal interference. However, 5GHz WLAN band is much larger than the notch bandwidth. Thus, we need to add another notch to target the upper part of WLAN band and enhance the filter performance for this application. In this case, we place a second SRR pair on the right side, without considering any geometrical modification on the feed line as usual. The SRR pair has the same basic shape with some customization in terms of dimensions and positioning shown in table III.4 and Figure III.15. So that the notch center is shifted to 5.8GHz rather than 5.2GHz.

Table III.4 dimensions of right SRR pair

Parameter	**A**	**B**	**C**	**D**	**E**	**G**
Dimension(mm)	3.95	3.2	0.30	0.30	0.40	0.42

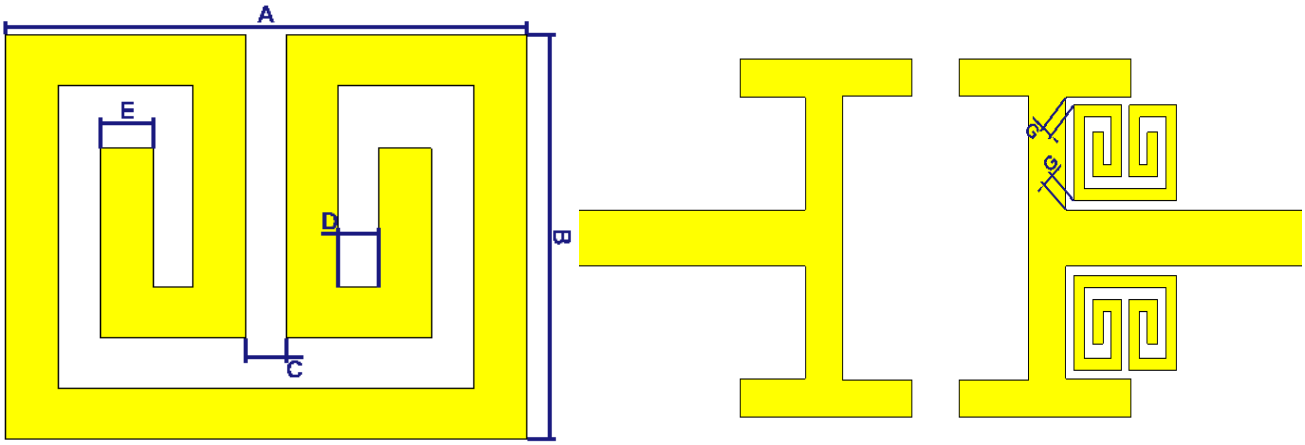

(a) (b)

Figure III.18 (a) Right SRR geometry (b) Right SRR positioning

Now we need to check whether both SRR pairs can be implemented on the same filter. For that purpose, we are going to analyze the notch response in two cases, where it is implemented alone, then combined with first one, based on the simulated S parameters of Figures III.16 and III.17.

The new notch should present high performance and neither affects nor get affected by the first one badly.

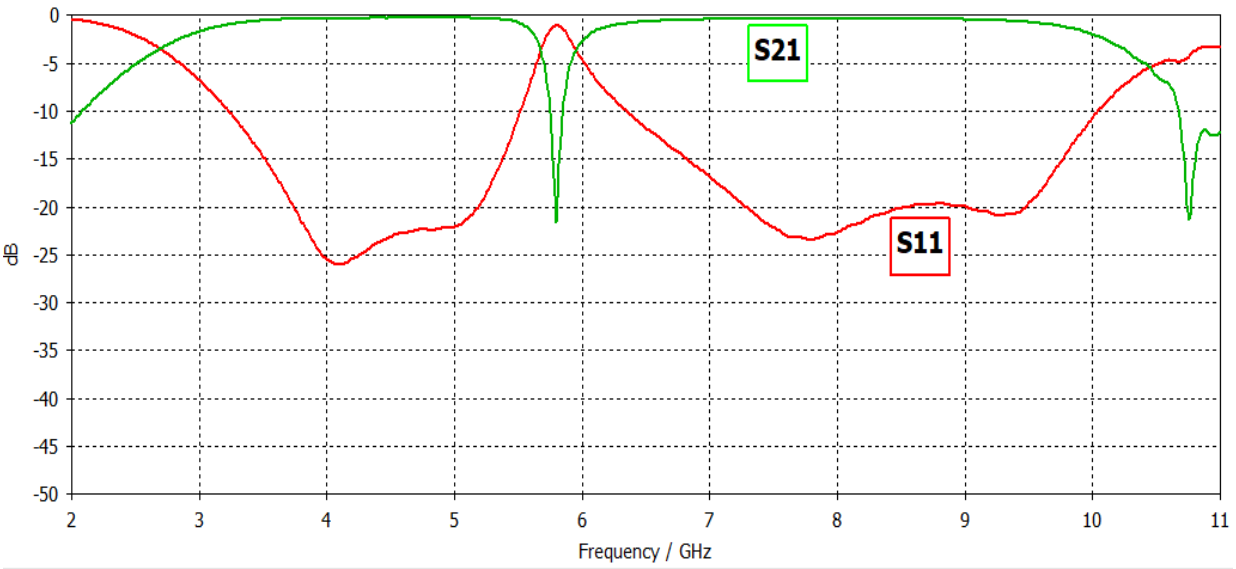

Figure III.19 Simulated S parameters for the right SRR pair

The above figure shows the response of the UWB BPF equipped with the right SRR pair only. The filter provides a flat pass band response for the entire UWB characterized by a -0.4dB insertion loss and around -20dB return loss. It is interrupted with a sharp notched band centered at 5.8GHz with less than -20dB insertion loss and a return loss approaching -0.8dB. The notch is 0.3GHz large ranging from 5.65GHz up to 5.95GHz, which cover the upper part of WLAN band with magnitude responses corresponding to our predefined criteria and a current distribution demonstrated below on figure III.20

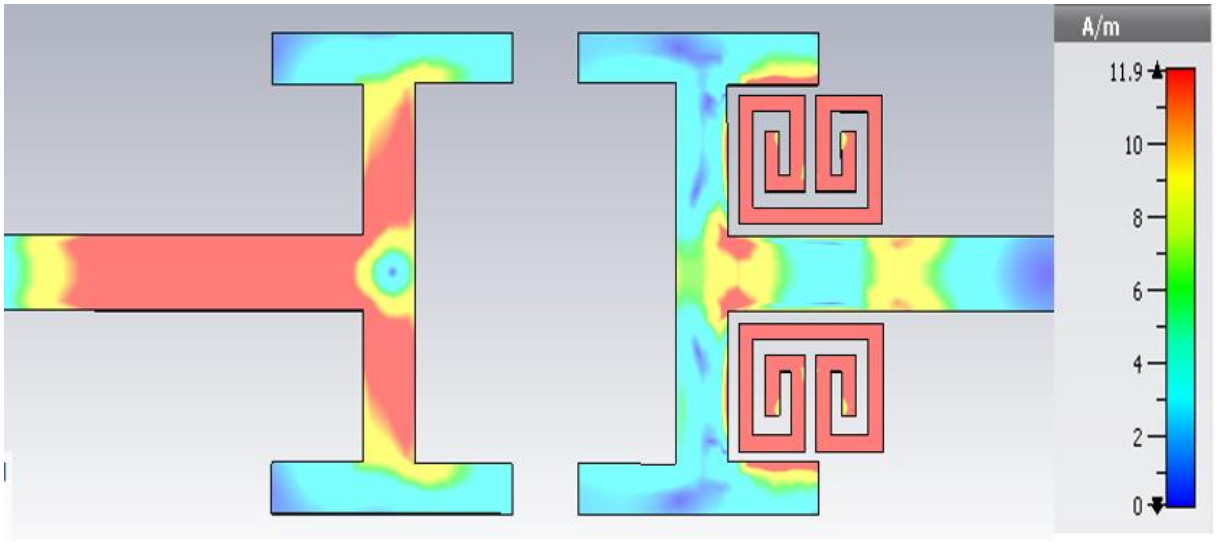

Figure III.20 current distribution at 5.8GHz

The above figure shows how current is distributed around the filter at 5.8GHz, where we can see a high density delivered by the input port through the feeding line, to be then concentrated completely around the SRR pair and prevented from passing to the output port as it is supposed to do.

The last step in designing the dual notched filter would be to check the interaction between the notches, by simulating the structure shown in figure III.18, which gave us the plots of figure III.19

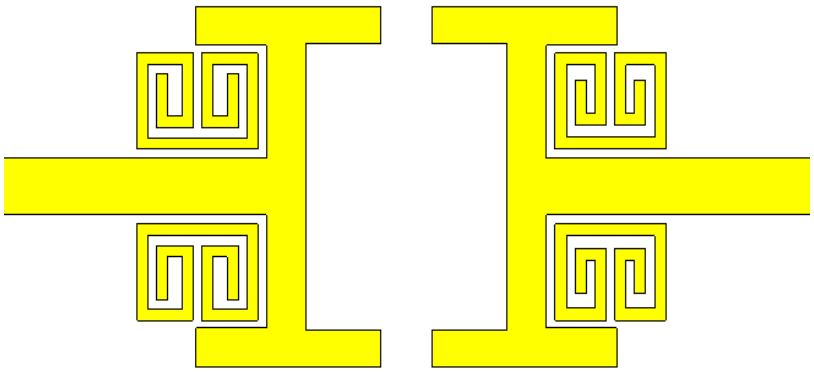

Figure III.21 Final dual notched filter design

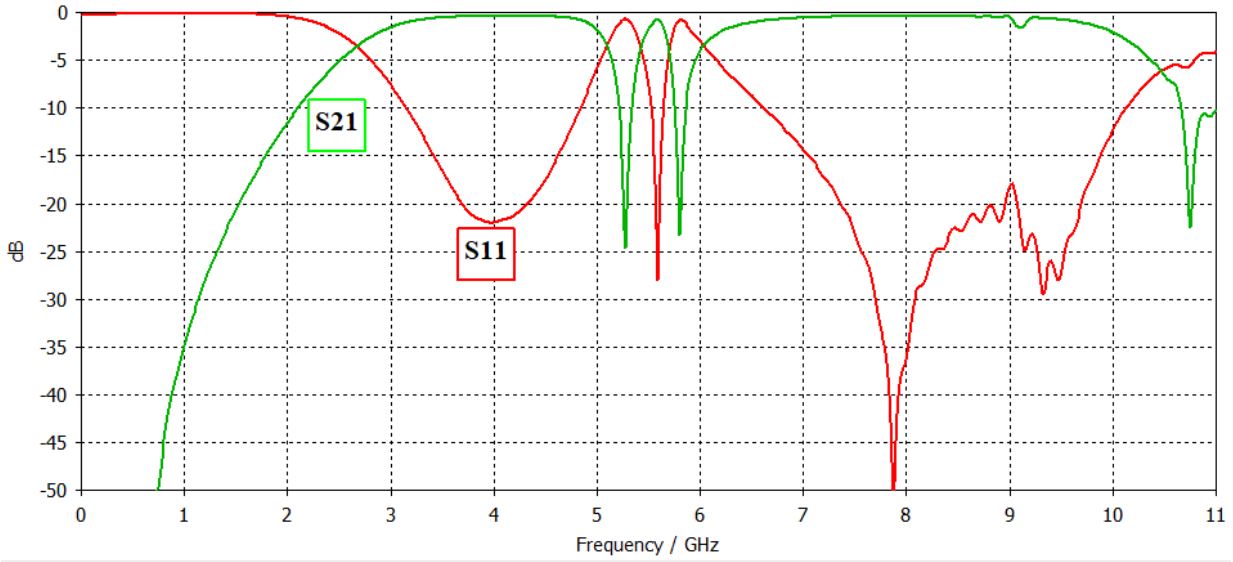

Figure III.22 Simulated S parameters for dual notched filter

The plot of figure III.22 displays the simulated return and insertion loss of the dual notched UWB BPF, where we have a response that fulfills the requirement with two sharp-notched bands at 5.2GHz and 5.8GHz, separated and surrounded by a pass band through the rest of the UWB. The notched bands are not affected by each other in terms of magnitudes or bandwidth except for a fluctuating return loss between 8GHz and 10GHz around -20dB, which falls within the acceptable range and the filter is valid for 5GHz WLAN band rejection.

III.3.4 Triple notched UWB BPF

As an addition to the dual notched filter structure, a third notch is introduced as follows:

A rectangular loop having the dimensions mentioned in table III.5 is added at the center of the filter. It is utilized in order to create a notch at 7.2GHz to eliminate interference with C-band satellite communication. Figure III.23 shows the proposed model while figure III.24 and III.25 demonstrates its frequency response in single and triple notch configuration respectively.

Table III.5 dimensions of the rectangular loop

Parameter	A	B	C	D
Dimension(mm)	5.30	6.50	8.90	0.45

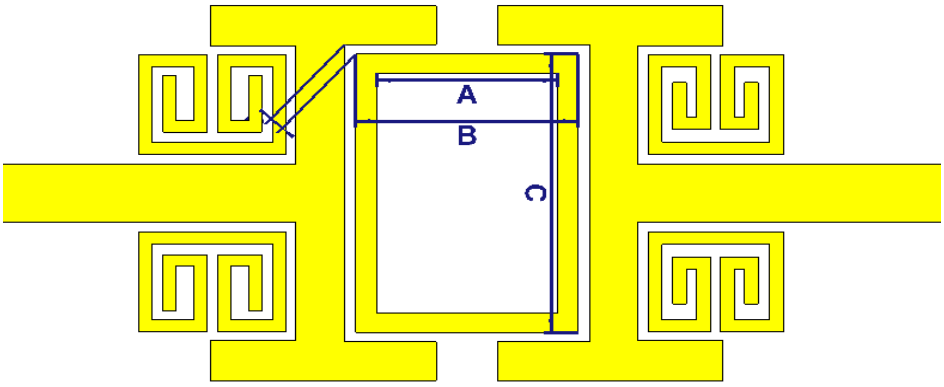

Figure III.23 Final triple notched filter design

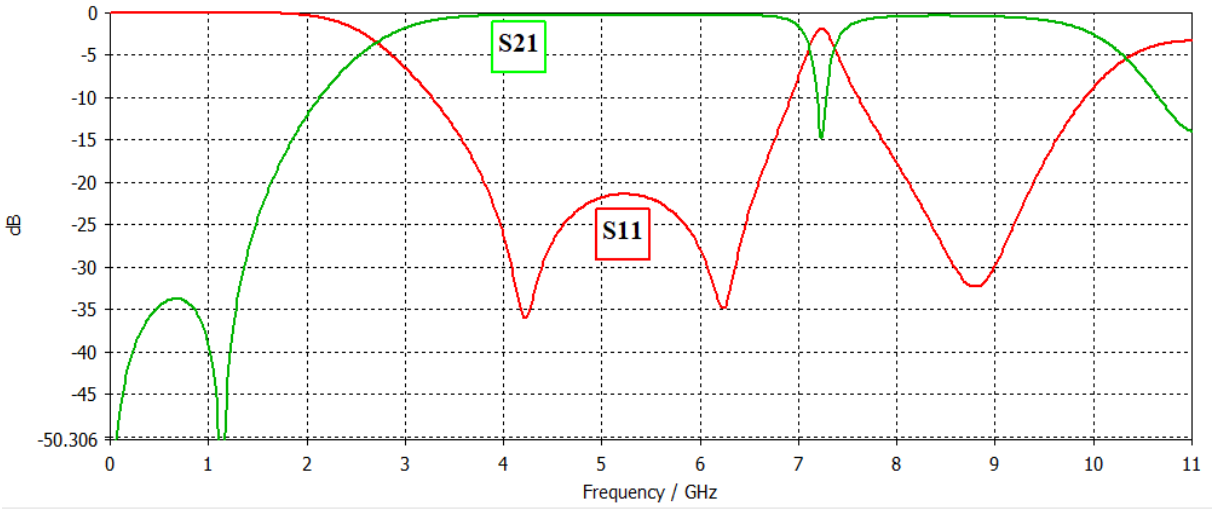

Figure III.24 Simulated S parameters for the third notch

Figure III.24 shows the filter response equipped only with the rectangular loop notch. As it is clearly seen, the filter provides a flat passband in the UWB range with a notched band at 7.2GHz characterized with an insertion loss of -15dB and a return loss approaching -1dB. The -3dB bandwidth is 0.25GHz centered at 7.2GHz, which falls within the acceptable parameters range, and makes the filter valid for C band application.

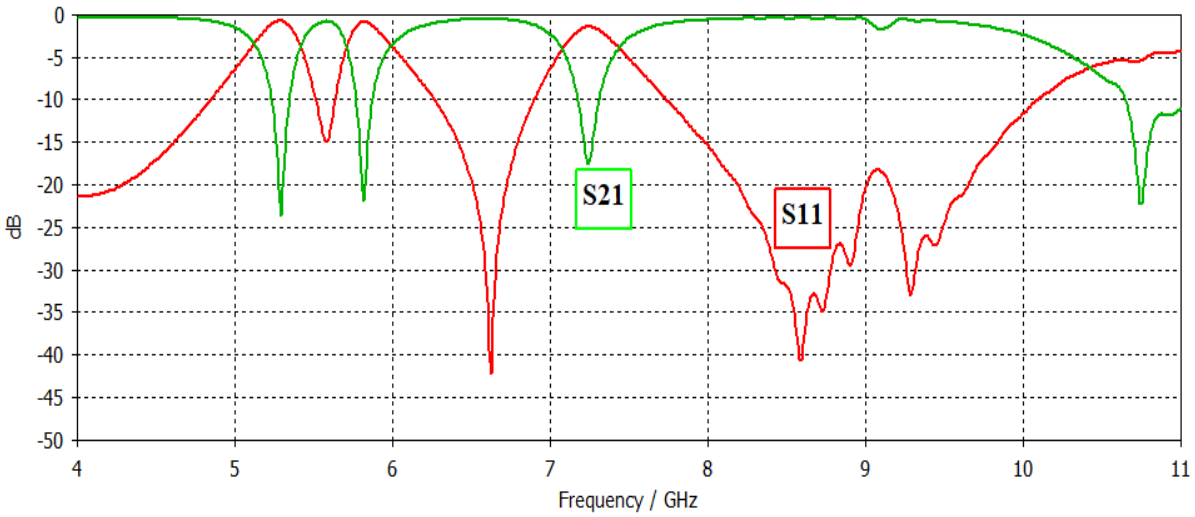

Figure III.25 Simulated S parameters for the triple notched filter

The above figure displays the response of our final triple notched filter design, where we can observe that notches do not affect or distort each other. Magnitudes of both IL and RL are within the acceptable range at the notched bands, surrounded with good pass band characteristics for the rest of UWB spectrum. Next, we have the current distribution around the structure at 7.20GHz

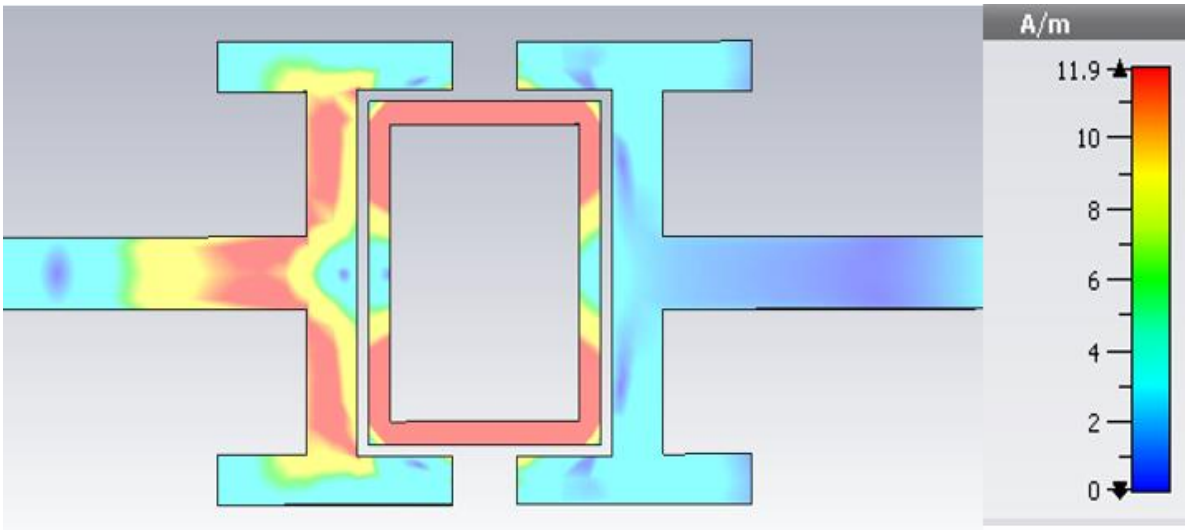

Figure III.26 Current distribution at 7.20GHz

The current distribution at the third notched band (7.2GHz) is demonstrated on figure III.26. A high current density concentrated around the rectangular loop, prevented from passing to the output port. The current distribution confirms the results discussed above.

One special characteristic of the rectangular loop notch is that it can be added or omitted without affecting the response of the filter. Means that the filter can be used as dual notched for WLAN application only. As it can be transformed into triple notched for WLAN and C band satellite applications just by opening and closing the rectangle as demonstrated on figure III.27.

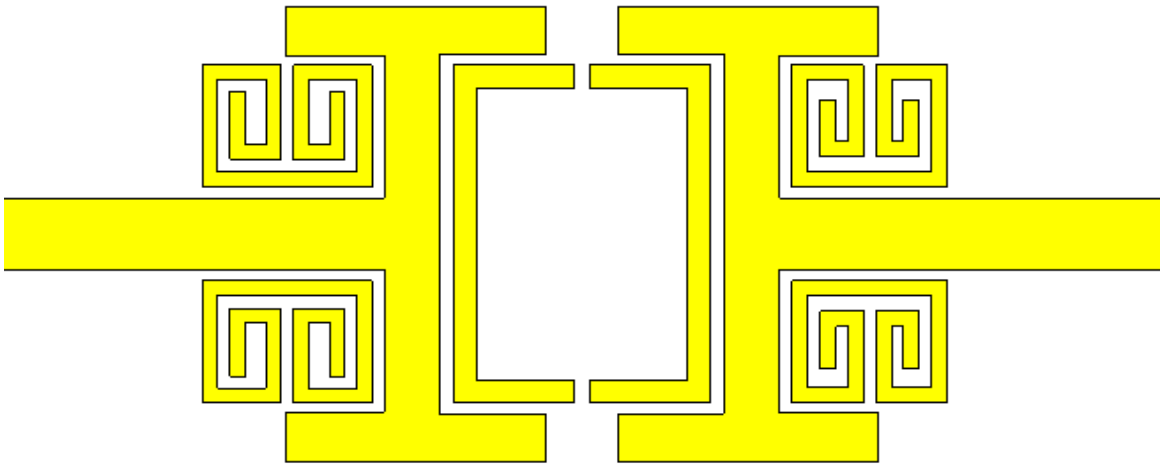

Figure III.27 Dual notched filter with open rectangle

The above structure leads us to the response displayed in figure III.22 as it omits the third notch and keep the rest unchanged.

III.4 Implementation and experimental results:

III.4.1 Implementation:

Our proposed UWB BPF filter is realized using MITS Electronics PCB prototyping machine, without and with dual notches to be measured and compared with the simulated results. Figure III.28 shows the prototyping machine while figure III.29 shows the top and bottom view alongside with dimensions of the fabricated filter and finally, figure III.30 demonstrates it with dual and triple notch configurations.

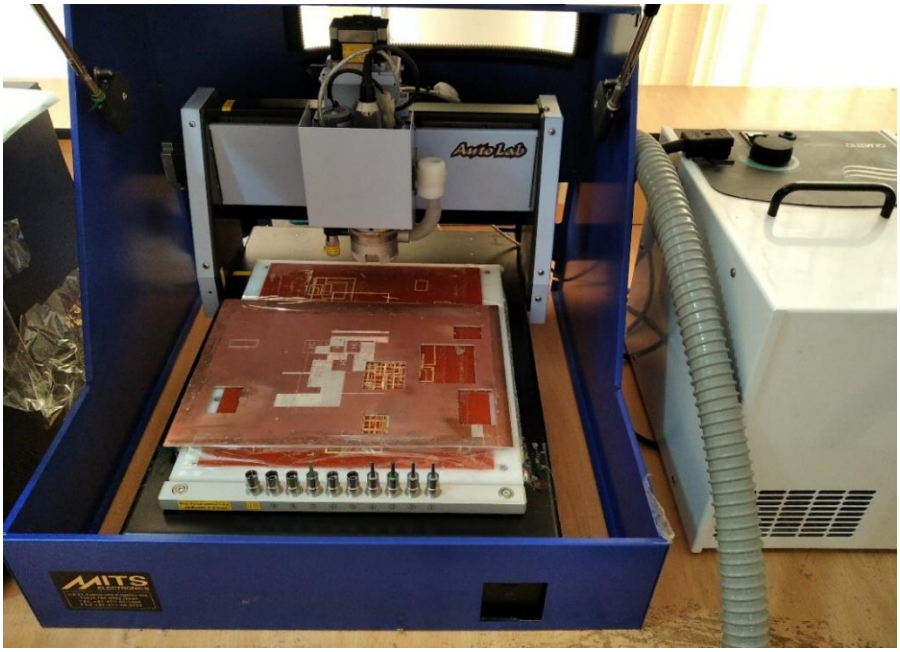

Figure III.28 MITS PCB prototyping machine

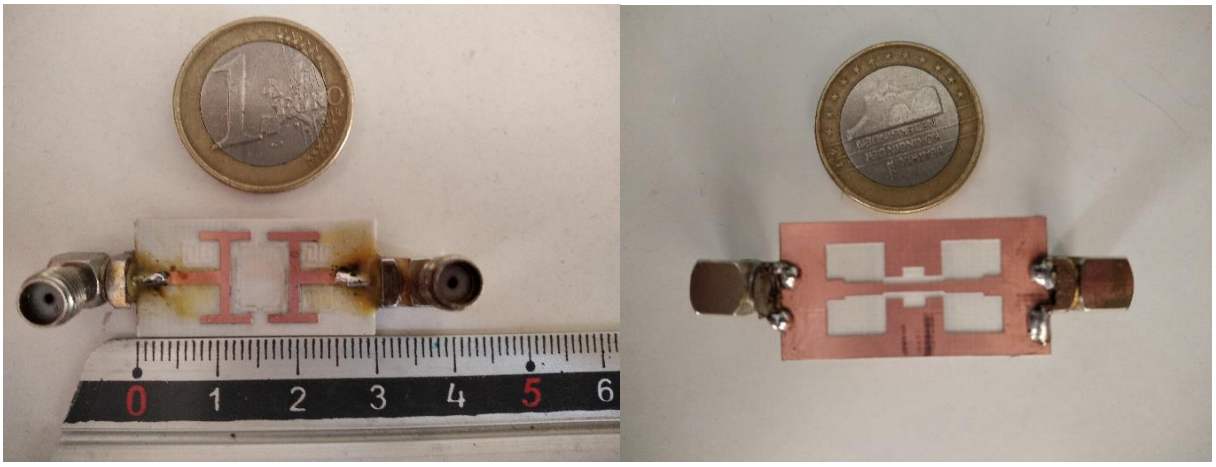

Figure III.29 UWB BPF (a) Top view (b) bottom view

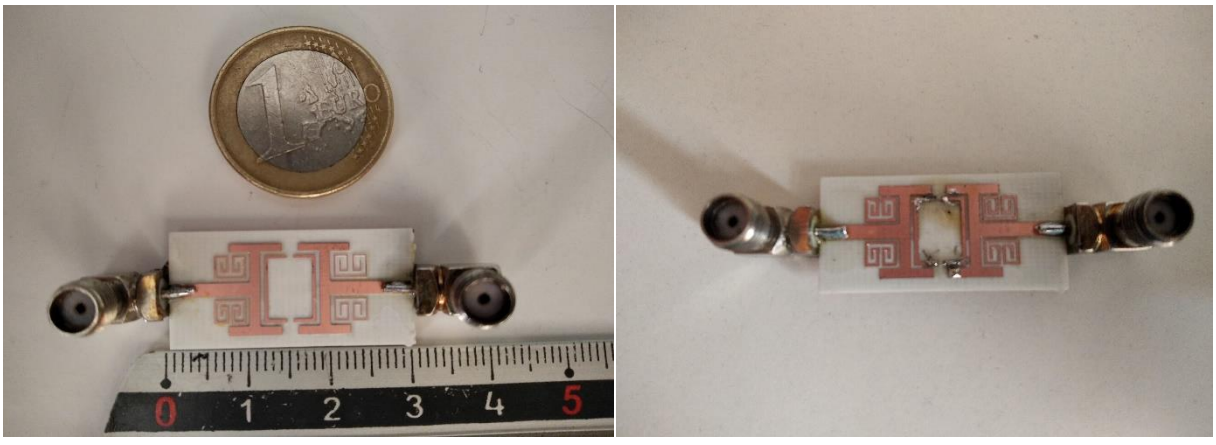

Figure III.30 UWB BPF (a) Dual notched (b) Triple notched

III.4.2 Experimental results

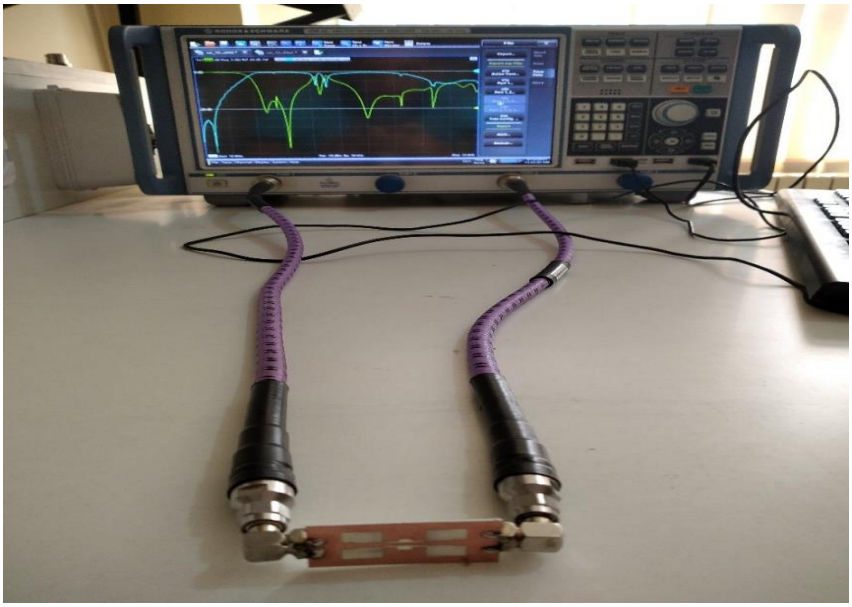

Figure III.31 Rohde & Schwarz VNA

After completing the fabrication process, we have measured each case of the filter response on Rohde & Schwarz VNA shown on the figure above. Figure III.32 display the BPF simulated (s) versus measured (m). Where we can notice an acceptable agreement for the 3.13GHz cutoff frequency and the insertion loss of -1dB for the fabricated filter. Which was not the case for the return loss that gave a fluctuating response between -10dB and -20dB followed by an extended bandwidth up to 11.3GHz compared to 10GHz for the simulated one.

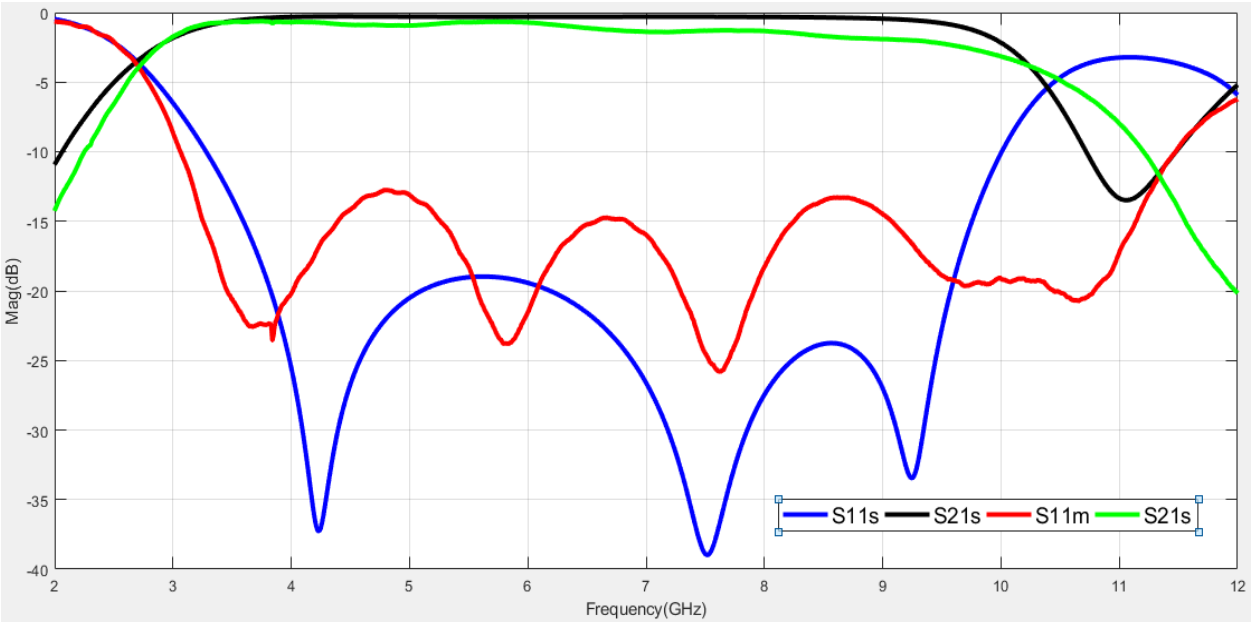

Figure III.32 simulated versus measured UWB BPF response

In the next step, we are going to compare the dual notched filter responses plotted below.

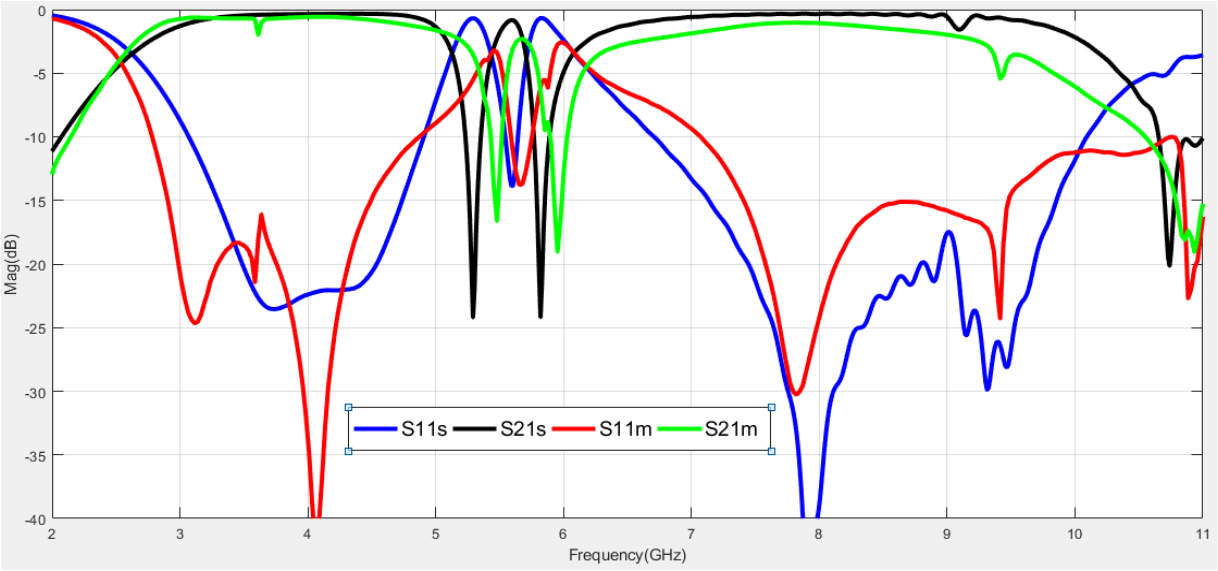

Figure III.33 simulated versus measured dual notched filter response

The figure represents a plot of the simulated and measured filter response in dual rejection mode where we see a noticeable amelioration compared to BPF. In this case, the responses agree well with each other in terms of general shape with small degradation of the insertion loss in addition to a shift 0.2GHz in frequency at the rejection bands due to the fabrication process and the frequency sensitivity of SRR's thickness.

Next, we close the rectangular loop using soldering as shown in Figure 3.30 (b), in order to get the final triple notched response displayed below

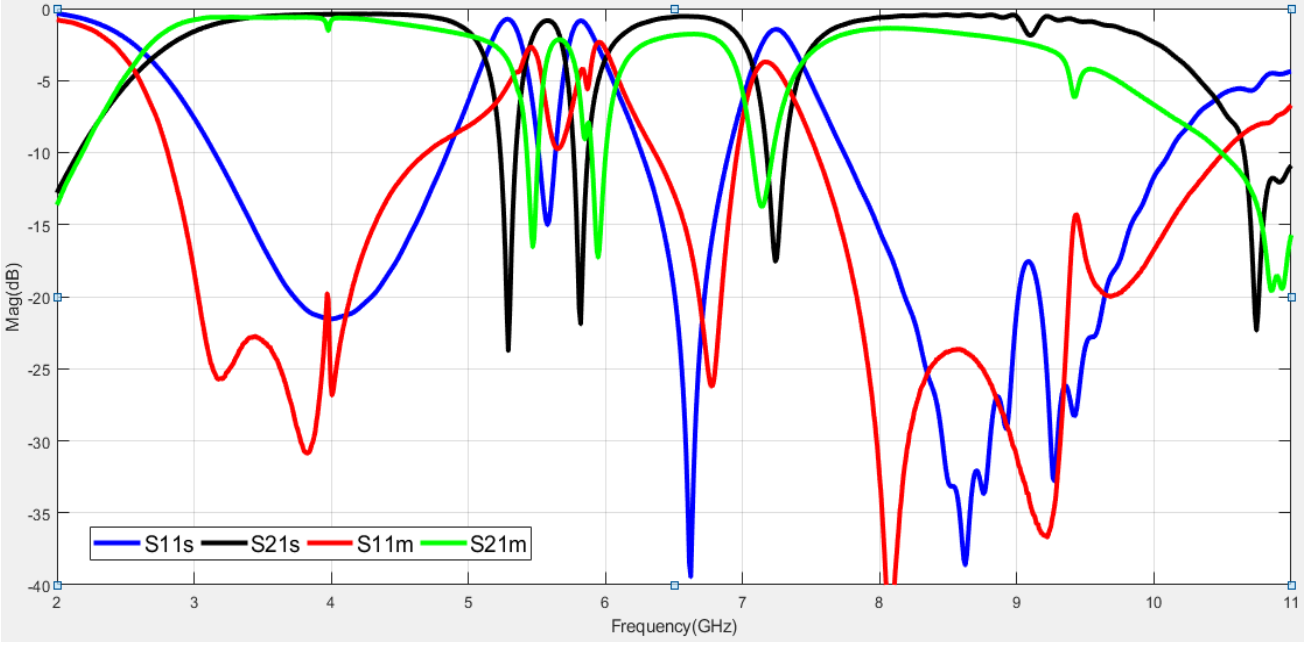

Figure III.34 simulated versus measured triple notched filter response

As described on figure III.34, the third notch performs well also with a small shift down in frequency of 20 MHz only where the rest of the response still the same as mentioned on figure III.33. In general, we had some shift in the rejection bands alongside minor deteriorations in terms of insertion and return loss which is caused by the accuracy of fabrication and soldering processes especially with a very thin substrate like ROGERS 4003 in addition to the insertion loss caused by SMA connectors. Finally, the table below summarizes a performance comparison of our simulated design versus similar works.

Table III.6 performance comparison between our design and other works

Ref	**h (mm)**	**Dielectric constant**	**Area (mm*mm)**	**BW (GHz)**	**Fn1| Fn2|Fn3 (GHz)**	**Fn1| Fn2|Fn3 Rejection level (dB)**
Ref. [36]	0.762	3.66	34x12	7.8	3.3|5.1|8.3	-28|-19|-15
Ref. [37]	1	3.55	25x10	6.9	5.8|8	-10|-15
This work	0.813	3.38	30x15	7.7	5.2|5.8|7.2	-23.8|-22|-17.5

Comparing our design to similar ones, it combines between compact size and a high rejection level at notch bands, in addition to an acceptable bandwidth close to the one on Ref. [36]

III.4.3 Adding switches

The aim of adding switches to the design is being able to activate and deactivate notches in order to pass or reject desired frequency bands. Three pairs of ideal switches S1, S2 and S3 are added to the structure at the positions indicated by the figure below

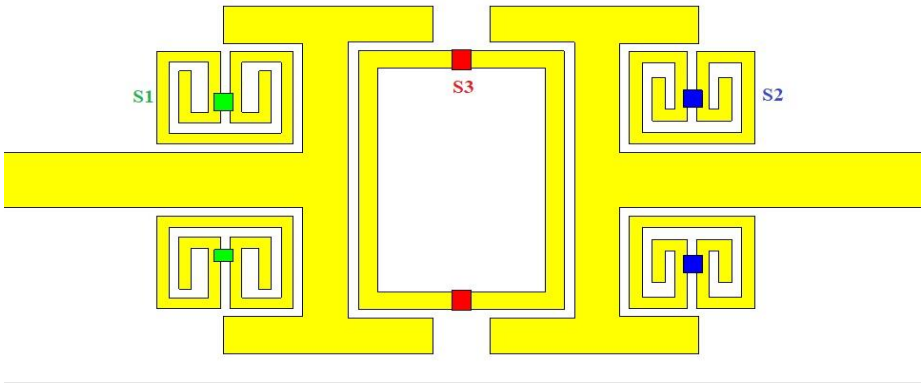

Figure III.35 Switches placement within the filter

The table below summarizes the eight possible switches configuration alongside with the filter operation in each case, an ON switch represents by the existence of a copper strip where its absence is represented by the OFF state. The effect SRR pairs is suppressed when the switch pair in ON, unlike the rectangular loop that generates the notch when the switch is ON. Examples of these possible reconfigurations are displayed on figures III.36 and III.37 to represent mode 5 and mode 8 respectively.

Table III.7 Switches configurations

Modes	S1	S2	S3	Operation	Stop band Frequencies
Mode 1	OFF	OFF	OFF	Dual notched filter	5.2GHz | 5.8GHz
Mode 2	OFF	OFF	ON	Triple notched filter	5.2GHz | 5.8GHz | 7.2GHz
Mode 3	OFF	ON	ON	Dual notched filter	5.2GHz | 7.2GHz
Mode 4	OFF	ON	OFF	Single notched filter	5.2GHz
Mode 5	ON	OFF	OFF	Dual notched filter	5.8GHz | 7.2GHz
Mode 6	ON	OFF	ON	Single notched filter	5.8GHz
Mode 7	ON	ON	OFF	UWB BPF	None
Mode 8	ON	ON	ON	Single notched filter	7.2GHz

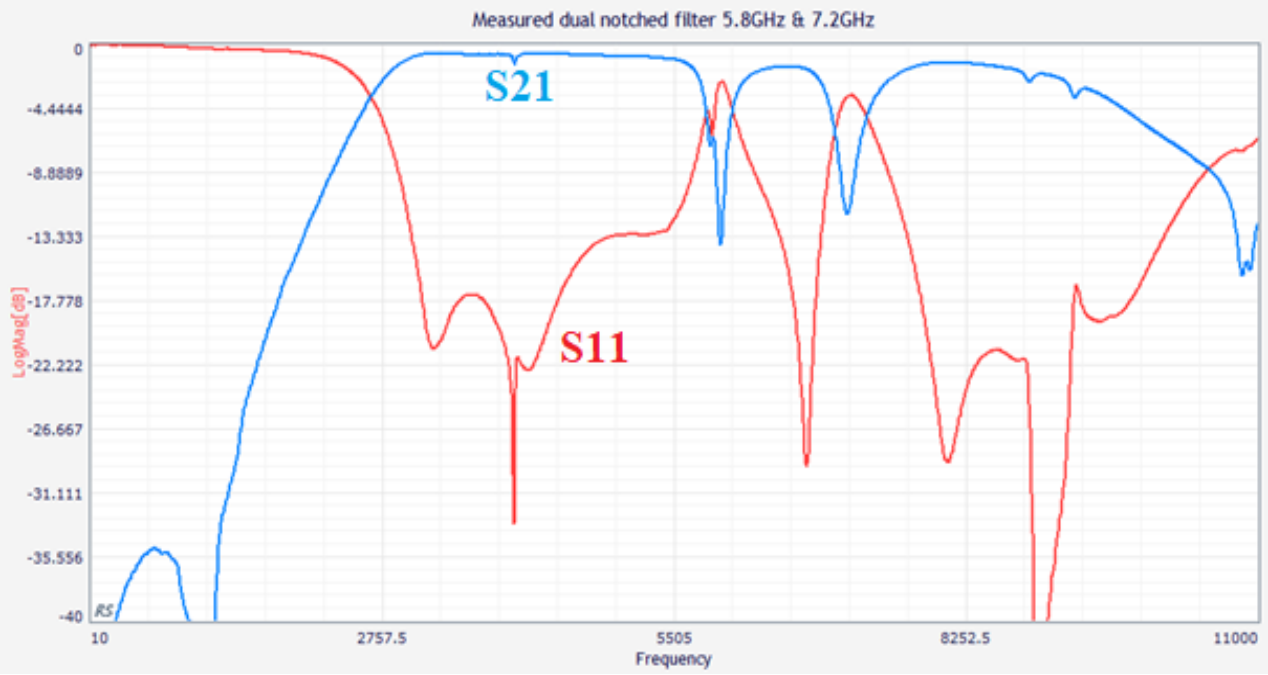

Figure III.36 measured response for mode 5 configuration

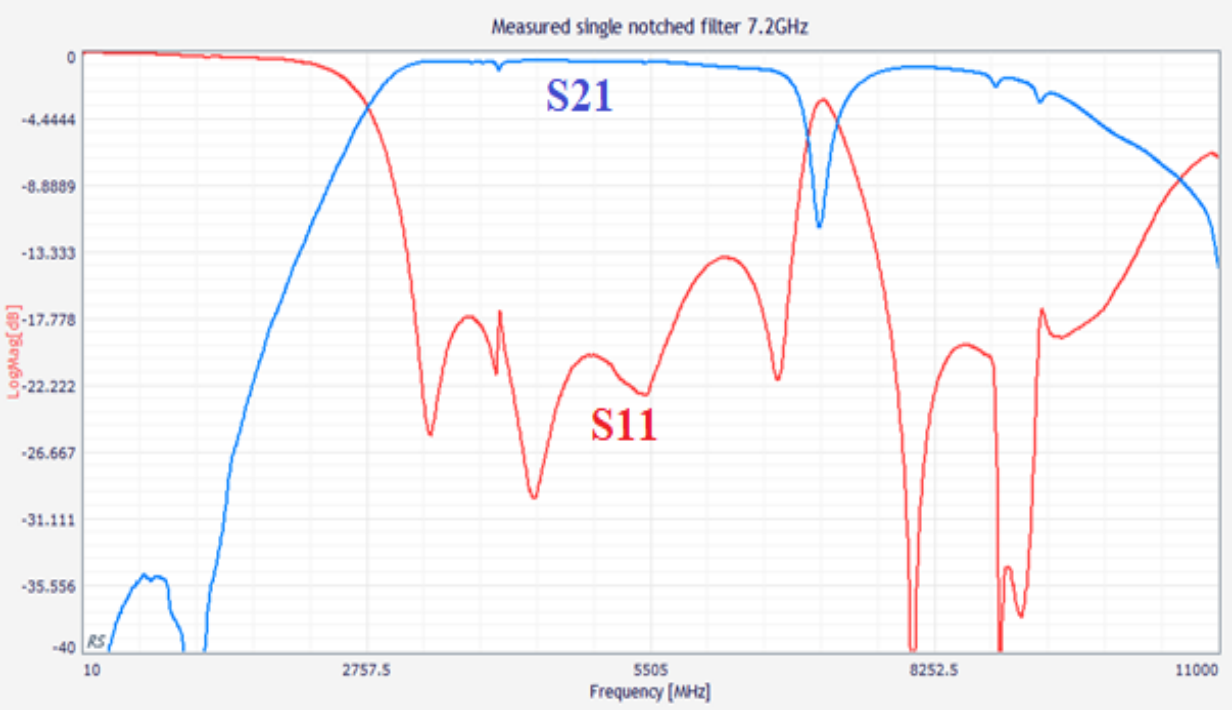

Figure III.37 measured response for mode 8 configuration

III.5 Conclusion

In this chapter, a miniaturized UWB BPF was proposed then optimized for the best achievable results before passing to the fabrication. The realized filter measurements gave a wide pass band of 8.2GHz ranging from 3.1GHz up to 11.3GHz, which meets the requirement of UWB. The filter is then equipped with two SRR pairs and rectangular loop at its center making it able to reject three bands used for two applications. 5.3GHz and 5.8GHz for WLAN in addition to 7.2GHz for C band which are common interfering signal with UWB technology.

General conclusion

In this work, a compact microstrip UWB BPF with multiple notches is designed, analyzed and implemented using ROGERS4003C substrate. The design and simulation are carried out using CST software. The fabrication and measurement are made using MITS Electronics and ROHDE & SCHWARZ VNA.

A literature review of microwave filters and DGS technique have been introduced in the first chapter. UWB technology in addition to development of UWB Bandpass Filters have been briefly presented in Chapter II. In the last chapter, an UWB BPF is proposed based on modified dumbbell shaped DGS, the structure provides an insertion loss around -0.4dB alongside with a return loss under -15dB for the pass band associated with a good suppression level outside the UWB. The filter is then equipped with two pairs of SRRs in order to create notched bands at 5.2GHz and 5.8GHz; in addition to a rectangular loop responsible of rejecting interferences caused by C band satellite communication signals at 7.2GHz at a high rejection level. After performing well, the design was then fabricated and measured to be finally compared with the simulated structure and other related works.

For further work, we propose:

- An investigation on reducing the filter size.
- Improving the sharpness and the bandwidth of the filter.
- Circuit modelling of the proposed filter.

Hopefully, this modest work will give some help for future filter applications.

References

[1] https://www.intechopen.com/books/uwb-technology-circuits-and-systems/review-on-uwb-bandpass-filters.

[2] K. Lacanette, "A Basic Introduction to Filters - Active, Passive, and Switched Capacitor," National Semiconductor Corporation, Application Note No. 779, retrieved from Texas Instruments, April 2010.

[3] Nadia Benabdallah, Nasreddine benahmed, Fethi Tarik Bendimerad, " Analysis and Design of an UWB Band pass filter wit Improved Upper Stop Performance". International Journal of Modern Engineering Research (UMER),2013.

[4] Vensa Crnojevié-Benjamin, " Advances in Multi-band Microstrip Filters, " IET Electromagnetic waves Series 48-ISBN 978-0-85296-777-5, Cambridge University press, 2006.

[5] David M. Pozar, " Microwave Engineering ", 4th ed., University of Massachusettes at Amherst; John Wiley & Sons, Inc, 2012.

[6] H. Miyake, S. Kitazawa, T. Ishizaki, T.Yamanda, and Y. Nagatomi, " A miniaturized monolithic dual band filter using ceramic lamination technique for dual mode portable telephones ", IEEE MIT-S int. Microwave symp.Dig., pp 789-792, June 1997.

[7] Standards Coordinating Committee, " IEEE Standard for Microwave Filter Definitions, " IEEE,20 may 2011.

[8] C. Quendo, E. Rius, and C. Person, " Narrow band-pass filters using dual behavior resonators based on stepped-impedance subs and different length stubs ", IEEE Trans. on Microwave Theory and Techniques, Vol. 52, No. 3, pp 1034-1044, March 2004.

[9] S. F. Adam, "Transmission Lines, Chapter 18" , in Microwave Theory +Applications, pp. 320-358.

[10] K. C. Gupta, R. Garg, I. Bahl +P. Bhartia, Microstrip Lines +Slotlines, Artech House Publishers, 2nd ed., 1996.

[11] I. Rosu, "Microstrip, Stripline, and CPW Design," RF Technical Articles, Bucharest, Romania, 2012.

[12] M.-J. Gao, L.-S. Wu +J. F. Mao, "Compact notched ultra-wideband bandpass filter with improved out-of-band performance using quasi-electromagnetic bandgap structure," Progress In Electromagnetics Research, vol. 125, pp. 137- 150, 2012.

References

[13] Gary Breed,. " An Introduction to Defected Ground Structures in Microstrip Circuits ", High Frequency Electronics Copyrights © 2008 Summit Technical Media. LLC.

[14] Radisic V ., Qian Y ., Cocciolo R., +Itoh T ., "Novel 2-D photonic Bandgap Structure For Microstrip Lines" . IEEE Microwave Guide Wave Lett. Vol. 8, pp. 69-71, Feb 1998.

[15] Ahn D., Park J.S., Kim C.S, Kim J., Qian Y . and Itoh T ., " A Design of the low-pass Filter Using the Novel Microstrip Defected Ground Structure ", in IEEE Transactions on Microwave Theory and Techniques, Vol 49, No.1, January 2001.

[16] Weng L.H., Guo Y.C., Shi X.W., and Chen X.Q., "An Overview on Defected Ground Structure", Progress in Electromagnetic Research B, Vol.7, 173-189, 2008.

[17] Zhenhai S. and Fujise M., "Bandpass Filter Design Based on LTCC and DGS", Asia Pacific Microwave Conf. Proc. APMC, Vol. 1, 2-3, 2005.

[18] Zhang Y.L., Hong W., Wu K., Et al., "Novel Substrate Integrated Waveguide Cavity Filter With Defected Ground Structure," IEEE Trans. Microwave Theory Tech., Vol. 53, No.4, 1280-1287, 2005.

[19] Debatosh Guha, Sujoy Biswas +Chandrakanta Kumar, " Printed Antenna Designs Using Defected Ground Structures: A Review of Fundamentals +State-of-the- Art Developments", Forum for Electromagnetic Research Methods +Application Technologies (FERMAT).

[20] Chirag Garg, Magandeep Kaur, " A Review of Defected Ground Structure (DGS) in Microwave Design", International journal of innovative research electrical, electronics, instrumentation +control engineering Vol. 2, Issue 3, March 2014 Copyright to IJIREEICE.

[21] M. K. Khandelwal, B. K. Kanaujia and S. Kumar, "Defected Ground Structure: Fundamentals, Analysis, and Applications in Modern Wireless trends," Hindawi publishing corporation – International journal of Antennas and propagation, vol. 20, p. 22,2017.

[22] Balalem, A., A. R. Ali, J. Machac, et al., "Quasi-elliptic microstrip low-pass filters using an interdigital DGS slot," IEEE Microwave Compon. Lett., Vol. 17, No. 8, 586–588, 2007.

[23] Xiao, J. K., S. W. Ma, +S. L. Zhang, "Novel compact split ring stepped-impedance resonator (SIR) bandpass filters with transmission zeros," Progress In Electromagnetics Research, PIER 21, 329–339, 2007.

References

[24] Parui, S. K. +S. Das, “Performance enhancement of microstrip open loop resonator band pass filter by defected ground structures,” Conf. Proc. IEEE Int. Workshop Antenna Technol. Small Smart Antennas Metamater. Applic., 483–486, 2007.

[25] Naghshvarian-Jahromi, M. +M. Tayarani, “Miniature planar uwb bandpass filters with circular slots in ground,” Progress In Electromagnetics Research Letters, Vol. 3, 87–93, 2008.

[26] I. Hunter, Theory +Design of Microwave Filters, 1st ed., The Institution of Engineering +Technology, London, United Kingdom, 2001.

[27] P. Mondal, H. Dey, A. Roy +S. K. Parui, "Design of UWB Bandpass Filter with WLAN Band Rejection by DMS in Stub Loaded Microstrip HPF," Journal of Communications Engineering +Networks, vol. 2, no. 1, pp. 50-54, 2014.

[28] A.-F. Sheta and I. Elshafiey, "Microstrip Ultra-Wide-Band Filter," PIERS.

[29] Y. Rahayu, T. A. Rahman, R. Ngah +P. Hall, "Ultra Wideband Technology and Its Applications," in 5th IFIP International Conference on Wireless +Optical Communications Networks, Surabaya, Indonesia, June 2008.

[30] B. Allen, T. Brown, K. Schwieger, E. Zimmermann, W. Malik, D. Edwards, L. Ouvry +I. Oppermann, "Ultra Wideband: Applications, Technology and Future perspectives," in International Workshop on Convergent Technologies (IWCT), Oulu, Finland, 2005.

[31] R.S.Kshetrimayum, “An introduction to UWB communication systems,” IEEE POTENTIALS, April 2009.

[32] S. Ullah, M.Ali, Md. A. Hussain +K. S. Kwak, "Applications of UWB Technology" , IEEE Transactions, vol.55, no.10, pp.2907-2914, Oct. 2007.

[33] C. Cansever, "Design of a Microstrip Bandpass Filter for 3.1-10.6 GHz Uwb Systems," Electrical Engineering +Computer Science – Master Thesis, Syracuse University, 2013.

[34] Chia-Chin Chong, Fujio Watanabe, +Hiroshi Inamura, “Potential of UWB technology for the next generation wireless communications,” IEEE Ninth International Symposium on Spread Spectrum Techniques +Applications, Manaus, Amazon, Brazil, August 2006.

References

[35] Q. Zhang, “Ultra-wideband impulse radio communication system design +prototyping”, Tennessee Technological University, USA.

[36] Abdul Basit, Muhammad I. Khattak, +Mu’ath Al-Hasan, “Design +Analysis of a Microstrip Planar UWB Bandpass Filter with Triple Notch Bands for WiMAX, WLAN, +X-Band Satellite Communication Systems”, Progress In Electromagnetics Research M, Vol. 93, 155–164, 2020.

[37] Omid Mousavi, Ahmad Reza Eskandari, Mohammad M. R. Kashani, +Mohammad Ali Shameli, “Compact UWB Bandpass Filter with Two Notched Bands Using SISLR +DMS Structure”, Progress In Electromagnetics Research M, Vol. 80, 193–201, 2019.